A TIME-VECTOR ANALYSIS OF THE FREE LATERAL OSCILLATION OF AN AIRPLANE

by

ALAN HILMAN LEE

B. S., Oregon State College
(1950)

SUBMITTED IN PARTIAL FULFILLMENT OF THE
REQUIREMENTS FOR THE DEGREE OF
MASTER OF SCIENCE
at the
MASSACHUSETTS INSTITUTE OF TECHNOLOGY
June 1954

Signature of Author _____
Dept. of Aeronautical Engineering, May 24, 1954

Certified by _____
Thesis Supervisor

Accepted by _____
Chairman, Departmental Committee on Graduate Students

A TIME-VECTOR ANALYSIS OF THE FREE LATERAL OSCILLATION OF AN AIRPLANE

by

ALAN HILMAN LEE

Submitted to the Department of Aeronautical Engineering on May 24, 1954, in partial fulfillment of the requirements for the degree of Master of Science.

ABSTRACT

This thesis presents a time-vector method for extracting the lateral stability derivatives of an airplane from its fixed-control, lateral oscillation. The method of analysis is based on the concepts of rotating vectors long used in the field of electrical engineering. Specifically, the relationships existing between the phases and the amplitudes of the multiple degrees of freedom, and their time derivatives and integrals, of a linearly oscillating system are time-invariant. That principle permits a complete analysis with the oscillation "frozen" at any chosen time.

The time-vector method of analysis can be applied to either the direct or the indirect stability problem.

1. It can be used to determine the phase and amplitude relationships between the multiple degrees of freedom of a lightly-damped, oscillating system when the stability derivatives are known.
2. It can be used to determine the stability derivatives of a lightly-damped, linearly oscillating system from transient flight records.

This report is concerned with the second application. The method is developed and then applied to the lateral oscillation of a fighter airplane. A number of advantages which are a result of the physical insight afforded by the graphical solution are enumerated.

Thesis Supervisor: E. E. Larrabee

Title: Assistant Professor of Aeronautical Engineering

May 24, 1954

Professor Leicester F. Hamilton
Secretary of the Faculty
Massachusetts Institute of Technology
Cambridge 39, Massachusetts

Dear Sir:

A thesis entitled "A Time-Vector Analysis of the Free Lateral Oscillations of an Airplane" is herewith submitted in partial fulfillment of the requirements for the degree of Master of Science in Aeronautical Engineering.

Respectfully yours,

Alan H. Lee

ACKNOWLEDGMENTS

I wish to express my appreciation to Prof. Larrabee for suggesting the subject of this thesis, and for his willing counsel when obstacles were encountered.

TABLE OF CONTENTS

LIST OF FIGURES

LIST OF TABLES

I. SUMMARY

This report presents a time-vector method for extracting the lateral stability derivatives of an airplane from transient flight data. The method has been developed from a consideration of the properties of rotating vectors. The relationships between the phases and amplitudes of the multiple degrees of freedom of a linearlly oscillating system are time-invariant. That fact forms the basis of the time-vector method.

The lateral oscillation of a fighter airplane was analyzed. The analysis and sample calculations are presented in the appendix. It was shown that relationships between the stability derivatives could be derived which were commensurate with the accuracy of the transient data. The lateral oscillation provided sufficient conditions to evaluate five of the seven lateral stability derivatives in terms of the other two. A reasonable estimate for two of the derivatives gave good results for the others. A similar analysis of the rolling-subsidence and the spiral modes presents the two additional conditions which are necessary to a unique solution for all derivatives.

The time-vector method of analysis is direct and easily applied. The graphical solution permits an insight into the physical character of the oscillation. That quality facilitates the detection and correction of any inconsistencies that may be present in the data.

II. INTRODUCTION

A. A Discussion of the Problem

This report considers the application of a time-vector method to the extraction of the lateral stability derivatives of an airplane from transient flight data. The problem of determining stability derivatives directly from dynamic flight tests has received considerable attention in recent years. A brief background of the subject follows:

The basis for the study of airplane dynamics was introduced by Bryan in 1911, Ref. 1. His mathematical description of the fixed-control motion of an airplane remains fundamentally unchanged.

The fixed-control motion of an airplane is mathematically described by six simultaneous, linear, differential equations with constant coefficients. The equations are written for axes that are fixed in the airplane. They are derived with the assumption of small disturbances from an equilibrium flight condition. By virtue of airplane symmetry and the restriction to small disturbances, the equations can be separated into two groups which describe the longitudinal and the lateral motions. The form of the lateral dynamic equations used in this report is presented on page 12 .

The constant coefficients in the differential equations are called stability derivatives. They represent a change in an aerodynamic force or moment along, or about, one of the stability axis due to a departure from equilibrium. Limitations to their use are discussed in texts on the subject; one such text is Ref. 2.

Accurate estimates of stability derivatives are essential in the design of an airplane in order to insure good flight characteristics. Those estimates must be based on aerodynamic theory and, where possible, wind-tunnel tests. It would be beneficial to the aerodynamicist if he were able to get a direct check on his estimates from dynamic flight tests. Until recently, the only practical check available was a comparison between a calculated and an actual flight response to a disturbance. That check was not positive since compensating errors in the derivatives could mask significant inaccuracies.

It should be noted that the lateral stability derivatives of a Bristol fighter were extracted from flight tests by British investigators in the 1920's, ref. 3. Some similar work was done in this country in the 1930's and early 1940's. However, those methods were very difficult to apply and hence were not used generally by aerodynamicists in industry.

The difficulties inherent in estimating stability derivatives accurately were significantly increased with the use of highly swept wings and the advent of transonic flight speeds. The need for methods of checking estimated derivatives by dynamic flight tests of the completed airplane became more acute. The correlation between theory and practice would permit improved estimates of stability derivatives for advanced designs.

Considerable research effort has been expended in recent years toward the development of methods for extracting stability derivatives and stability performance functions from dynamic flight tests. Milliken has discussed some of the results obtained at the Cornell Aeronautical Laboratories in Refs. 4 and 5. A method developed at that installation

and applied in Ref. 6 is considered briefly in this report. The NACA has devoted considerable effort to the problem. Various methods developed in their laboratories are presented in Ref. 7 through 11. There are many other papers relating to the subject. The reader is referred to the more extensive bibliographies contained in the referenced documents.

This report is concerned principally with a time-vector method for extracting stability derivatives from transient flight data. The method is especially applicable to lightly-damped, oscillating systems. It is applied herein to the extraction of the lateral stability derivatives of a fighter airplane by analyzing its lateral oscillation.

The rotating vector diagram employed in the method has been used by electrical engineers for many years. The first known application in aeronautics was by Mueller of MIT in 1937, Ref. 12. He used it to determine the character of the longitudinal oscillatory modes of an airplane when its stability derivatives and inertia properties were known. Thus, he used it in the sense of synthesis. The principle lay dormant for many years. It has been considered by several people since World War II. Doetsch, a German scientist working in Great Britain, has prepared a report, Ref. 13, in which he considers an application similar to Mueller's in greater detail. He also applies the method in a synthesis sense.

The time-vector principle has been recently applied in the sense of analysis: the problem of determining the stability derivatives when the transient motion of the airplane is known. The only thorough development

and application of the method known to the writer was that of Professor Larrabee of MIT in Ref. 14. The development in this report closely follows that of Professor Larrabee.

B. Nomenclature

b	wing span, ft
C. G.	airplane center of gravity location, % M. A. C.
C_{L_o}	equilibrium lift coefficient
C_{ℓ_β}	$\frac{2}{\rho V_o^2 Sb} \frac{dL}{d\beta}$
C_{ℓ_p}	$\frac{2}{\rho V_o^2 Sb} \frac{dL}{d(pb/V_o)}$
C_{ℓ_r}	$\frac{2}{\rho V_o^2 Sb} \frac{dL}{d(rb/2V_o)}$
$C_{\ell_{\delta_a}}$	$\frac{2}{\rho V_0^2 Sb} \frac{dL}{d\delta_a}$
C_{n_β}	$\frac{2}{\rho V_o^2 Sb} \frac{dN}{d\beta}$
C_{n_p}	$\frac{2}{\rho V_o^2 Sb} \frac{dN}{d(pb/2V_o)}$
C_{n_r}	$\frac{2}{\rho V_o^2 Sb} \frac{dN}{d(rb/2V_o)}$
C_{y_β}	$\frac{2}{\rho V_o^2 Sb} \frac{dY}{d\beta}$
D	$\frac{d}{d(t/\tau_o)}$
g	acceleration due to gravity, 32. 2 ft/sec^2
i	$\sqrt{-1}$
I_{x_p}	airplane principal moment of inertia about the X-axis
I_{z_p}	airplane principal moment of inertia about the Z-axis
K_x^2	$\left[g/b^2 w \left(I_{x_p} \cos^2\eta + I_{z_p} \sin^2\eta \right)\right]$
K_z^2	$\left[g/b^2 w \left(I_{z_p} \cos^2\eta + I_{x_p} \sin^2\eta \right)\right]$

K_{xz}	$g/b^2 w \left(I_{z_p} - I_{x_p} \right) \sin \eta \cos \eta$
L	rolling moment, ft-lbs
M	Mach number
M. A. C.	mean aerodynamic chord, ft
N	yawing moment, ft-lb
n_y	lateral acceleration in g's
OAT	outside air temperature, ^oF
p	angular velocity about X-axis, rad/sec
r	angular velocity about Z-axis, rad/sec
S	wing area, ft^2
t	time, sec
V_c	calibrated airspeed
V_i	indicated airspeed
V_o	equilibrium true airspeed
W	gross weight, lb
Y	side force, lb
α	angle of attack, deg
β	angle of sideslip, rad
γ_o	flight path angle, rad
δ	pressure ratio, ambient/sea level
δ_a	total aileron angle, deg
e_D	$\sin^{-1}\zeta$, damping angle, rad
ϕ	angle of roll, deg

Φ_p	phase angle of p relative to β, deg
Φ_{n_y}	phase angle of n_y relative to β, deg
Φ_r	phase angle of r relative to β, deg
λ_p	rolling subsidence mode root
λ_s	spiral mode root
μ_o	$\frac{m}{\rho_o sb}$, airplane density parameter
η	angle between principal axis and stability axis
ω	angular velocity of oscillation, rad/sec
ω_n	undamped natural frequency, rad/sec
$'\omega_n$	$\tau_o \omega_n$, nondimensional undamped natural frequency
ρ_o	NACA std. sea level atm. density, slugs/ft^3
σ	atm. density ratio, ambient/sea level
τ_o	$\frac{b}{V_o \sqrt{\sigma}}$, aerodynamic time reference, sec
θ_{o_L}	airplane reference axis angle of zero lift, deg
ψ	angle of yaw, rad
ζ	lateral oscillation damping ratio

III. THEORY AND DISCUSSION

A. Properties of Rotating Vectors

Consider a freely oscillating system composed of a mass, a viscous damper, and a spring. For small disturbances, its motion can be described mathematically by a linear, second-order differential equation.

$$m \frac{d^2x}{dt^2} + \frac{dx}{dt} + k\,x = 0$$

where

x = displacement

m = mass

c = damping constant

k = spring constant

If the damping of the system is less than critical, the roots of the equation may be expressed as

$$\lambda = -\zeta\omega_n \pm i\omega_n \sqrt{1 - \zeta^2}$$

With initial conditions which eliminate one root,

$$x = x_o\, e^{-\zeta\omega_n t + i\omega_n \sqrt{1 - \zeta^2}\; t}$$

The first derivative of x can be written:

$$\frac{dx}{dt} = \left(-\zeta + i\sqrt{1 - \zeta^2} \right) \omega_n\, x$$

$$= \omega_n \left| x \right| e^{i(\Phi_x + 90^o + \epsilon_D)}$$

where ϵ_D = damping angle

$$= \tan^{-1} \frac{\zeta}{\sqrt{1 - \zeta^2}}$$

$$= \sin^{-1} \zeta$$

Similarly,

$$\int x \, dt = \frac{|x|}{\omega_n} e^{i(\Phi_x - 90^\circ - \epsilon_D)}$$

Those quantities can be plotted as vectors in the complex plane.

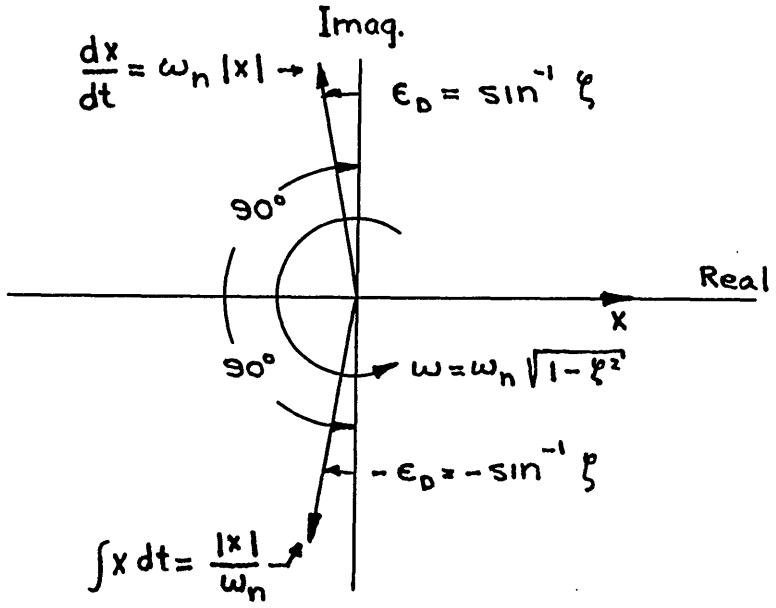

Fig. 1, Derivatives and Integrals of Vectors

The quantity x, its time-derivatives, and its integrals all rotate with the same angular velocity, ω, in the complex plane. Also, each of the vectors has its magnitude decreased by the same multiplicative factor, $e^{-\zeta\omega_n t}$. It follows that the relationships existing between the amplitudes and phases of the vectors are not functions of time.

For the simple mass-spring-viscous damper system described by the equation

$$m\ddot{x} + c\dot{x} + kx = 0,$$

oscillatory solutions can be represented by closure of a vector in which each of the terms is represented by a vector as shown in Fig. 2.

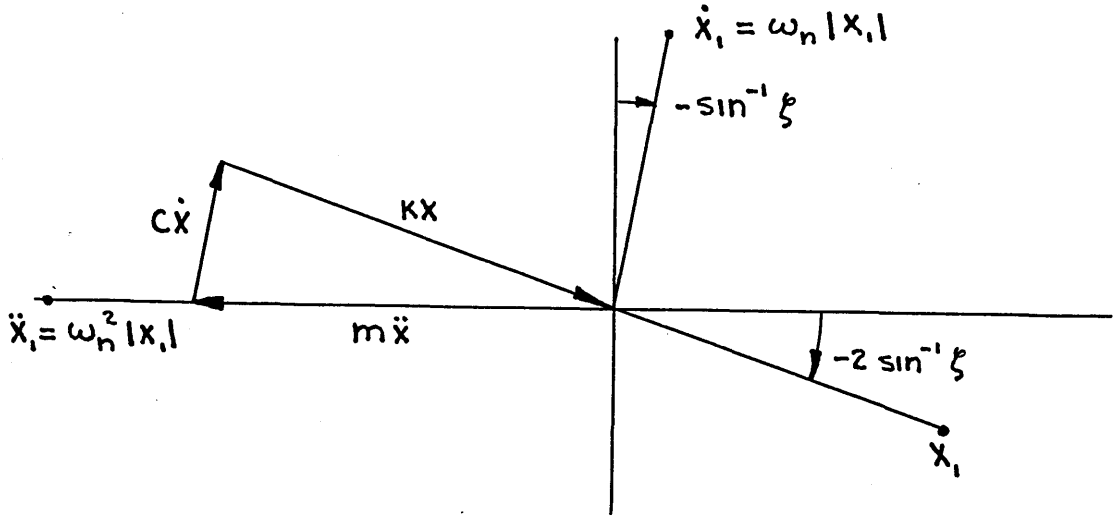

Fig. 2, Vector solution for one-degree-of-freedom oscillation

The concepts established for the one-degree-of-freedom system can be extended directly to a system, with multiple degrees of freedom. All components of the system, and all derivatives and integrals of the components, will rotate with the same angular velocity and decay with time by the same factor. Hence, phase and amplitude relationships between the components of a linearly oscillating, multiple-degree-of-freedom system are time-invariant. That conclusion is important; it is the foundation of the time-vector method for analyzing oscillating systems. The phase and amplitude relationships between the components to comprising the motion may be determined by considering the oscillation frozen at any

instant. The relationships may be used to solve for the constant coefficients of the linear differential equations which describe the complete oscillation.

B. Application of the Principle to Airplane Lateral Dynamics Analysis

This report considers the application of the method to the short period, lateral oscillation of an airplane. The relatively light damping of that motion makes it especially susceptible to time-vector analysis.

The differential equations which describe the fixed-control, lateral motion of an airplane are presented below.

$$(2\mu_o K_x^2 D^2 - \frac{\sqrt{\sigma}}{2} C_{\ell_p} D)\phi + (2\mu_o K_{xz} D^2 - \frac{\sqrt{\sigma}}{2} C_{\ell_r} D)\psi - (C_{\ell_\beta})\beta = 0$$

$$(2\mu_o K_{xz} D^2 - \frac{\sqrt{\sigma}}{2} C_{n_p} D)\phi + (2\mu_o K_z^2 D^2 - \frac{\sqrt{\sigma}}{2} C_{n_r} D)\psi - C_{n_\beta})\beta = 0$$

$$-(C_{L_o})\phi + (2\mu_o D - C_{L_o} \tan \gamma_o)\psi + (2\mu_o D - C_{y_\beta})\beta = 0$$

The form of the equations corresponds to NACA practice.

It is noted that a total of seven stability derivatives in the equations are unknown. It is of interest to consider the number which may be evaluated uniquely by analyzing the lateral oscillation.

The instrumentation recommended for lateral oscillation testing includes provisions to measure the rate of roll, the rate of yaw, and the lateral acceleration. The flight test records then yield information concerning the ratios:

1. $|p| : |r| : |n_y|$
2. $\Phi_p : \Phi_r : \Phi_{n_y}$

Those ratios provide four known conditions which permit the solution of four of the unknown derivatives in terms of the other three. The side force equation, as written, assumes that sideslip is the only means of generating a side force. With that condition, the side-force derivative can be evaluated from a nondimensional form of Newton's Second Law of Dynamics,

$$C_{y_\beta} \beta = C_{L_o} n_y$$

It also follows that the phase angles of β and n_y differ by 180^o. The side force assumption is excellent for conventional aircraft. If an unusually large vertical tail is employed, the contribution of roll rate and yaw rate to the side force should be investigated.

In the usual case, the lateral oscillation, with the side-force assumption, provides sufficient information to determine five of the seven unknown stability derivatives. In order to evaluate them uniquely, the magnitudes of two derivatives must be estimated or obtained from another source. It may be possible to separate the rolling subsidence mode and the spiral mode from the lateral oscillation. If so, they will provide the two additional conditions necessary for a unique solution of all derivatives. That possibility will be discussed later in the report.

C. Transient Analysis

The first step in analyzing a transient is to determine:

1. the frequency of the oscillation,

2. the damping ratio,

3. the relationship between the amplitudes of the degrees of freedom,

4. the relationship between the phase angles of the degrees of freedom.

That information can be obtained by plotting the oscillation data in the following manner:

First, plot the times at which all components of the oscillation cross the zero axis as shown in Fig. 3.

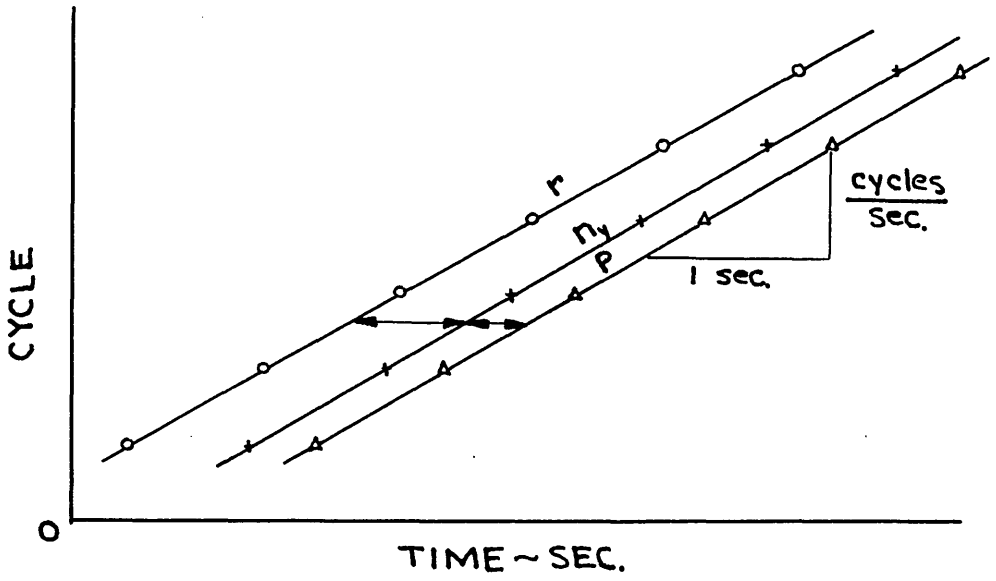

Fig. 3, Frequency Plot

The common slope of the curves of Fig. 3 precisely determines the frequency and the period of the oscillation. The horizontal distance between the curves provides the relationship between the phase angles of the degrees of freedom. The data points for each oscillatory component

should generate a straight line. If they do not, it is an indication that nonlinearities are present.

The second graph should have the logarithms of the maximum amplitudes of the oscillation plotted versus their times of occurrence.

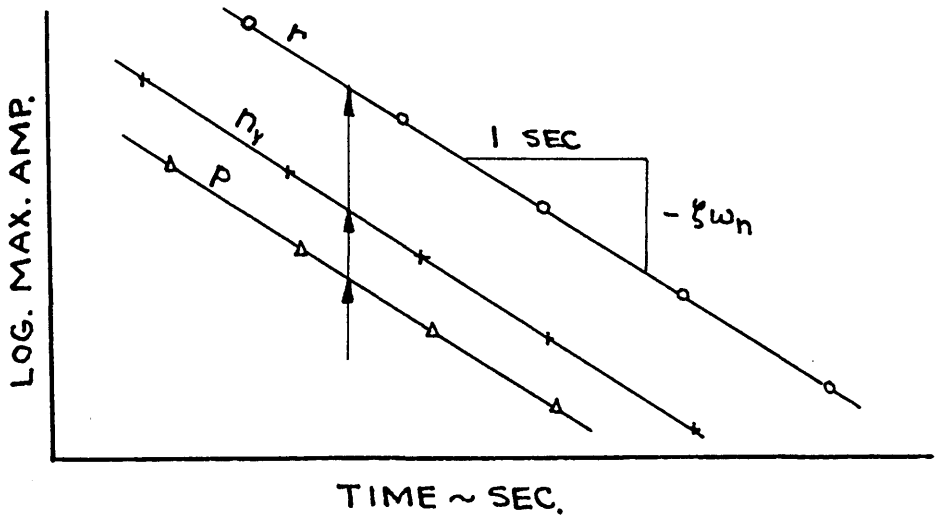

Fig. 4, Amplitude Plot

The slope of the curves of Fig. 4 establishes the damping of the motion. The decay of the vectors of Fig. 1 was shown to be represented by:

$$x = Ce^{-\zeta\omega_n t}$$

$$\ln x = \ln C - \zeta\omega_n t$$

and

$$\zeta\omega_n = \frac{\ln C - \ln x}{t} \qquad (1)$$

where C = max. amp. at t = 0

x = max. amp. at t = t.

Also recall that

$$\omega = \omega_n \sqrt{1 - \zeta^2} \qquad (2)$$

The values of the damping ratio (ζ) and the undamped natural frequency (ω_n) can be solved with relations (1) and (2).

The relative amplitudes of the degrees of freedom may be ascertained by considering the motion frozen at any instant. The amplitude relationships may be determined along vertical lines as shown in Fig. 4.

Misalignments of the rate instrument input axes and improper location of the lateral accellerometer have significant effects on the measured phase and amplitude relationships. When those conditions exist, corrections must be applied to the data. A method of correcting phase and amplitude relationships for instrument geometry is given on page 24 .

The corrected data can be presented as a vector diagram in the complex plane. The general appearance will be that of Fig. 5. It was shown that measuring β is usually unnecessary. The phase of β can be considered to differ from that of n_y by 180^o. The nagnitude of β can be established by the side-force vector diagram. That is indeed fortuitous since sideslip is inherently difficult to measure accurately.

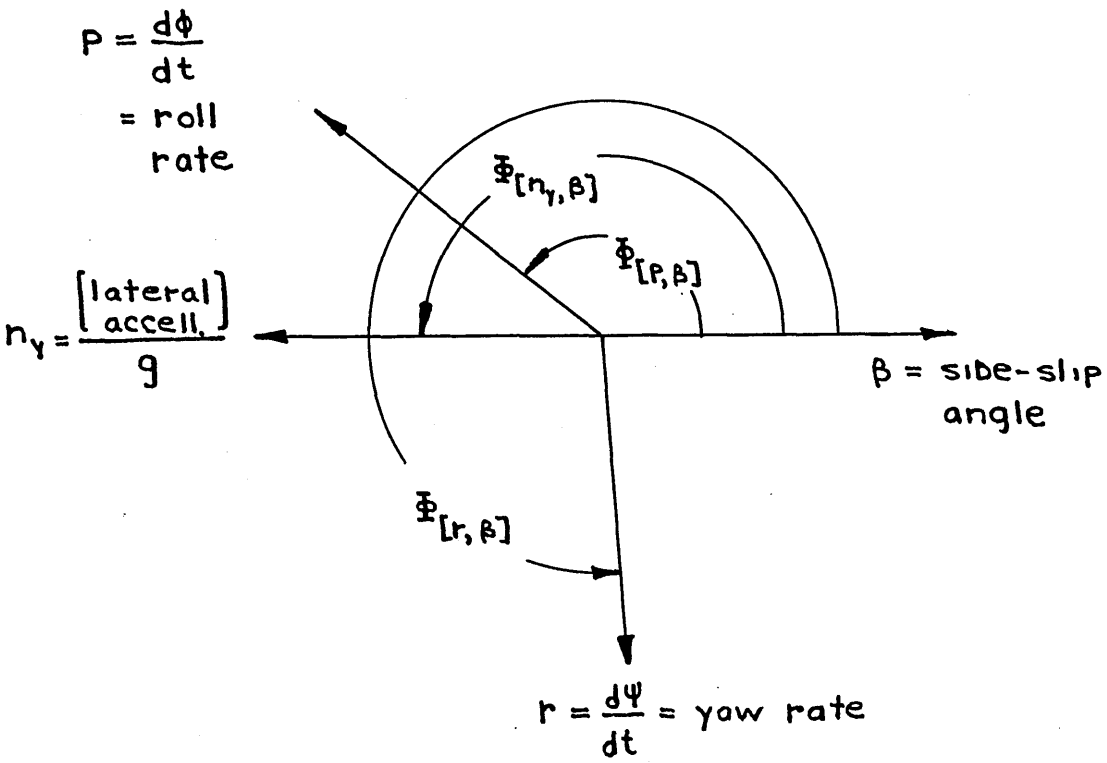

Fig. 5, Vector Diagram of Oscillation Components

D. Construction of the Vector Diagrams

It is convenient to consider the side-force equation first. It may be written as

$$\frac{2\mu_o}{\sqrt{\sigma}} D\beta = C_{Y_\beta}\beta + C_{L_o}\phi - \frac{2\mu_o}{\sqrt{\sigma}} D\psi$$

Construction of the side-force diagram facilitates critism of the transient data. The magnitudes of all terms on the right hand side of the equation are known. It is not uncommon for the vector diagram to fail to close. The appropriate adjustment is to alter the phase of r with respect to β

and n_y as required. The employment of identical rate gyros for the roll and yaw freedoms will minimize the phase distortion between those components. However, some phase distortion can be expected between the rate gyros and the accellerometer. The phase distortion considered here is of a random nature. The instrument dynamics should be known before they are installed in the airplane.

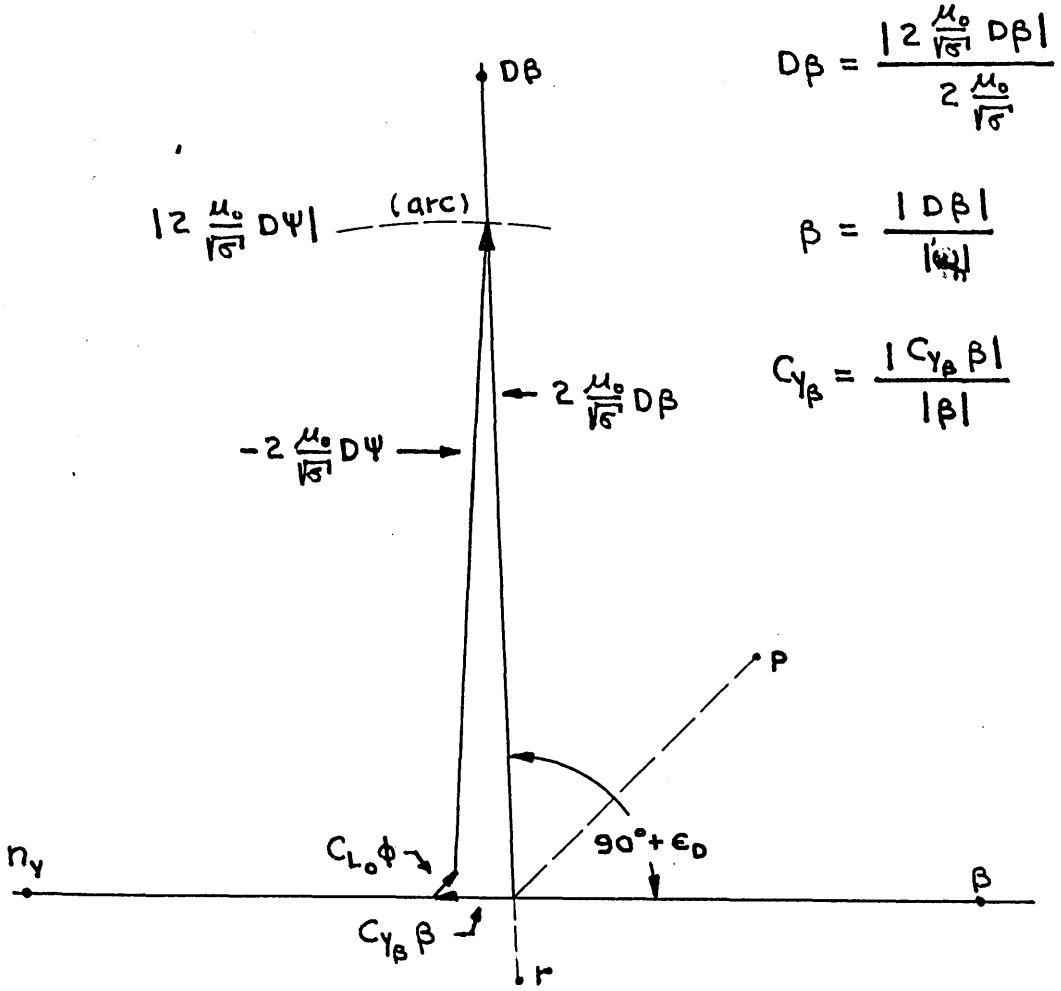

Fig. 6, Side-Force Vector Diagram

The side-force diagram has yielded:

1. consistent relationships between the phases and amplitudes of r, n_y, and β;

2. the magnitude of C_{y_β};
3. an opportunity to criticize the accuracy of the phase and amplitude data.

The rolling-moment equation may be considered next. It is convenient to write it:

$$2\mu_o K_x^2 D^2\phi - \frac{\sqrt{\sigma}}{2} C_{l_r} D\psi + 2\mu_o K_{xz} D^2\psi = \frac{\sqrt{\sigma}}{2} C_{l_p} D\phi + C_{l_\beta}\beta$$

One of the three unknown stability derivatives must be estimated or obtained from another source. The proper derivative to estimate will depend upon the airplane configuration. C_{l_r} was considered estimated in the equation above and in the diagram of Fig. 7.

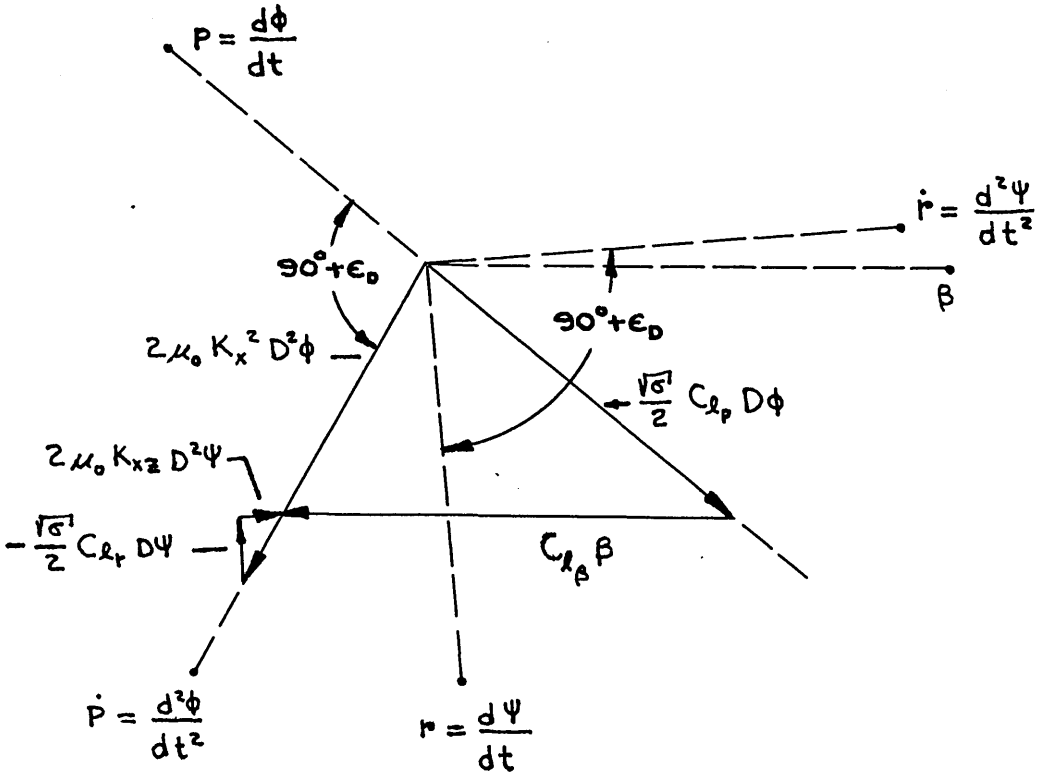

Fig. 7, Rolling-Moment Vector Diagram

$$C_{\ell_p} = \frac{-\left|\frac{\sqrt{\sigma}}{2} C_{\ell_p} D\phi\right|}{\left|\frac{\sqrt{\sigma}}{2} D\phi\right|}$$

$$C_{\ell_\beta} = \frac{\left|C_{\ell_\beta} \beta\right|}{|\beta|}$$

Accurate phase relationships between the degrees of freedom are essential for good results. If an improbable value is obtained for C_{ℓ_p} (which can be estimated with reasonable accuracy), it is probably an indication of a small error in the phase of the roll rate, p. In that event, the best estimate of C_{ℓ_p} should be inserted into the vector diagram. The rolling-moment diagram then yields:

1. a good value for C_{ℓ_β};
2. an improve phase relationship for p with respect to β.

All improved phase relationships should be used in subsequent diagrams.

The yawing-moment equation may be written:

$$2\mu_o K_z^2 D^2\psi + 2\mu_o K_{xz} D^2\phi - \frac{\sqrt{\sigma}}{2} C_{n_r} D\psi = \frac{\sqrt{\sigma}}{2} C_{n_p} D\phi + C_{n_\beta} \beta$$

Again, one of the three unknown derivatives must be estimated in order to permit a unique evaluation of the other two. The easiest derivative to estimate depends upon the airplane configuration. C_{n_r} was estimated in Fig. 8.

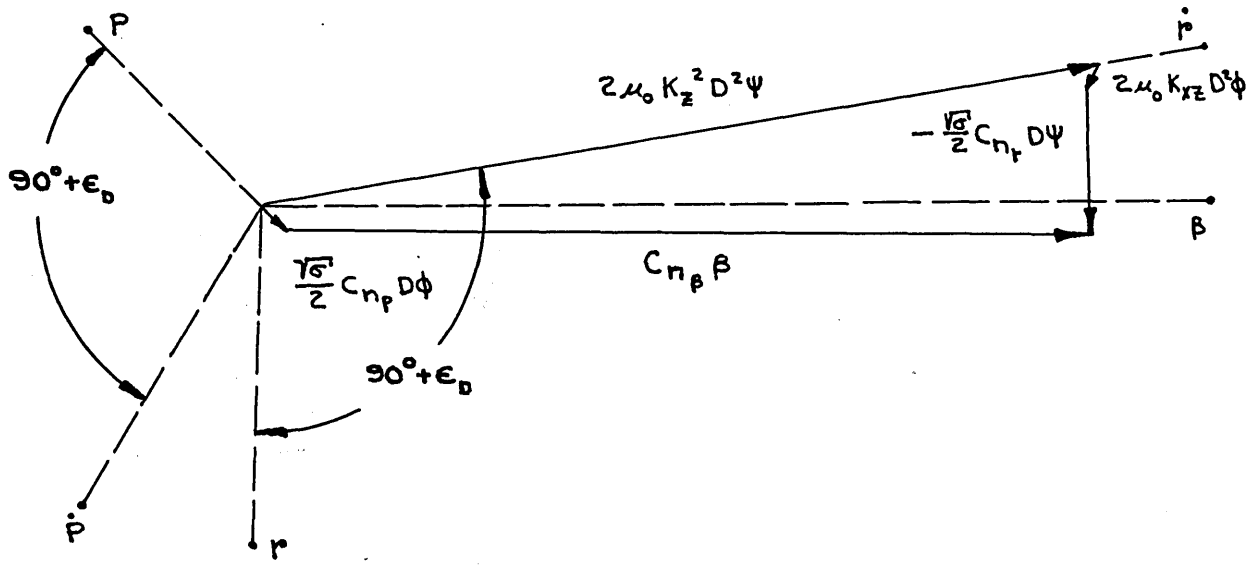

Fig. 8, Yawing-Moment Vector Diagram

$$C_{n_p} = -\frac{\left|\frac{\sqrt{\sigma}}{2} C_{n_p} D\phi\right|}{\left|\frac{\sqrt{\sigma}}{2} D\phi\right|}$$

$$C_{n_\beta} = \frac{|C_{n_\beta}\beta|}{|\beta|}$$

The yawing-moment diagram has yielded:

1. the magnitude of C_{n_p};
2. the magnitude of C_{n_β};

An important feature of the time-vector method of transient analysis should not be overlooked. Since it is a graphical solution, it permits a visual consideration of the relative importance of the oscillation components. The graphical constructions are easily checked by slide-rule

calculations.

Data inconsistencies are easily discovered. The physical insight afforded by the vector diagrams facilitates logical adjustments.

E. Consideration of the Rolling-Subsidence and the Spiral Modes

It has been noted that it is not possible to evaluate all of the lateral stability with the lateral oscillation. Two derivatives had to be estimated or obtained from another source. In some cases, it is possible to separate the rolling-subsidence and spiral modes from the lateral oscillation in the flight record. If that can be accomplished, those modes will supply the additional conditions necessary for a unique solution of all derivatives. The difficulty lies in the accurate identification of the modes which is essential to a good solution of their roots.

The rolling-subsidence mode may be extracted by back-figuring the oscillations after their linear parameters have been established. The difference between the record and the calculated motion is due to the rolling-subsidence mode as shown in Fig. 9.

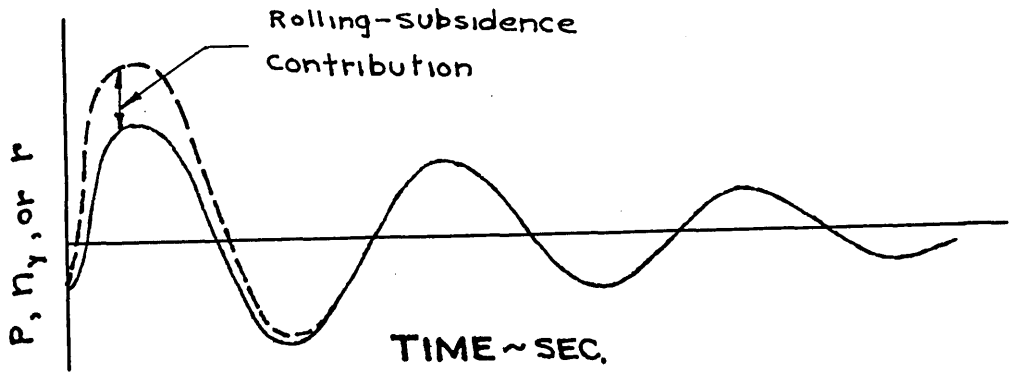

Fig. 9, Rolling-Subsidence Mode Separation

The rolling-subsidence mode principally consists of a heavy damping of the roll rate. As such, it is most easily identified in the roll rate record.

The general nature of the motion may be used to get an approximate expression for the rolling-subsidence root. By neglecting the relatively unimportant terms, it can be written as:

$$\lambda_r \cong \frac{\frac{\sqrt{\sigma}}{2} C_{\ell_p}}{2\mu_o K_x^2} \left(1 - \frac{C_{n_p} C_{\ell_\beta}}{C_{n_\beta} C_{\ell_p}} \right)$$

$$= \frac{b}{\text{Time to 1/e initial amplitudes}} \times V_o \sqrt{\sigma}$$

= spans flown to 1/e initial amplitudes.

When λ_r and the ratio p:r:β of the rolling subsidence mode have been determined, they may be inerted into the roll equation as:

$$-2\mu_o K_x^2 \left(\frac{b}{V_o\sqrt{\sigma}}\right)^2 \lambda_r p - \frac{\sqrt{\sigma}}{2} C_{\ell_p} \left(\frac{b}{V_o\sqrt{\sigma}}\right) p -$$

$$-2\mu_o K_{xz} \left(\frac{b}{V_o\sqrt{\sigma}}\right)^2 \lambda_r r - \frac{\sqrt{\sigma}}{2} C_{\ell_r} \left(\frac{b}{V_o\sqrt{\sigma}}\right) r - C_{\ell_\beta} \beta = 0$$

That provides another relation between C_{ℓ_p}, C_{ℓ_r}, and C_{ℓ_β}

It should be noted that λ_r and the ratio p:r:β are also time-invariant throughout the maneuver. Then

$$u = u_o e^{-\lambda t}, \qquad \frac{du}{dt} = -\lambda u_o e^{-\lambda t}$$

and $\int u\,dt = \frac{u_o}{\lambda} e^{-\lambda t}$.

The spiral mode is easily identified if the oscillation is allowed to continue for a sufficient period. However, the time required to develop a reasonable amplitude is usually so great the atmospheric turbulence becomes a significant factor. Since the motion grows or subsides so slowly, it is advisable to measure roll angles and headings since

$$\phi = \frac{p}{\lambda_s} , \qquad \psi = \frac{r}{\lambda_s} .$$

The spiral root and the ratio $p:r:\beta$ may be inserted into the yawing-moment equation to give another relationship between C_{n_p}, C_{n_r}, and C_{n_β}.

An approximate functional relationship may be written for λ_s as:

$$\lambda_s \cong \frac{\sqrt{\sigma}}{2} \frac{C_{L_o}}{\mu_o} \frac{C_{\ell_r}}{C_{\ell_p}} \frac{\left(1 - \frac{C_{n_r} C_{\ell_\beta}}{C_{n_\beta} C_{\ell_r}}\right)}{\left(1 - \frac{C_{n_p} C_{\ell_\beta}}{C_{n_\beta} C_{\ell_p}} + 2\mu_o K_z^2 \frac{C_{L_o} C_{\ell_\beta}}{C_{n_\beta} C_{\ell_p}}\right)}$$

$$= \frac{b}{\text{Time to e initial amplitudes if unstable}} \times \frac{V_o}{\sqrt{\sigma}}$$

$$=$$ spans flown to e initial amplitudes.

F. Corrections for Instrument Orientations and Locations

Roll rates and yaw rates should be measured about the airplane stability axes; lateral accelleration should be measured at the airplane center of gravity normal to the plane of symmetry. The usual flight test

instrumentation has the accellerometer aligned in the proper direction. It is often impractical to fulfill the other conditions.

The X-stability axis is initially aligned with the equilibrium flight direction; its relationship to the airplane center line is a function of airplane angle of attack. It would not be practical to make frequent changes in the roll rate and yaw rate instrument orientations.

The airplane center of gravity may not be accessible for instrument installation. For example, it may be located inside a fuel cell. In that event, the lateral accellerometer should be located as near to the airplane center of gravity as is possible.

The measured quantities may be corrected for instrument geometry as shown below

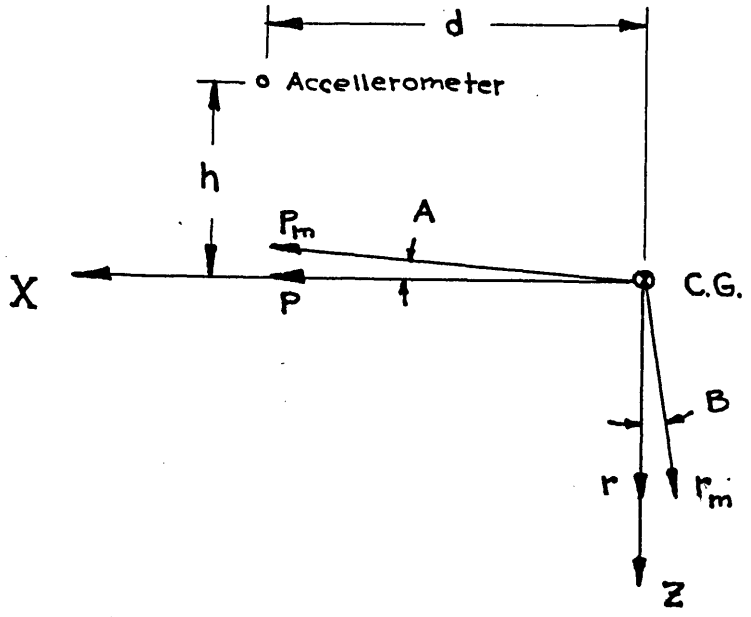

Fig. 10, Instrument Orientation Diagram

From Fig. 10,

$$n_y = n_{y_m} - \frac{h}{g}\dot{p} - \frac{d}{g}\dot{r}$$

where

$$\dot{p} = \frac{d^2\phi}{dt^2}$$

$$\dot{r} = \frac{d^2\psi}{dt^2}$$

$$p = p_m \cos A - p_m \sin B$$

$$p = p_m \cos B - p_m \sin A$$

Since each quantity is identified by a phase and an amplitude, its expression in terms of complex variables facilitates combination.

$$P = |P_m| \cos A \, e^{i\Phi_{P_m}} - |r_m| \sin B \, e^{i\Phi_{r_m}}$$

$$= \left(|P_m| \cos A \cos \Phi_{P_m} - |r_m| \sin B \cos \Phi_{r_m}\right) +$$

$$+ i\left(|P_m| \cos A \sin \Phi_{P_m} - |r_m| \sin B \sin \Phi_{r_m}\right)$$

$$= |P| e^{i\Phi_P}.$$

The yaw rate can be treated similarly to yield

$$r = |r| e^{i\Phi_r}$$

Now recall that

$$\dot{p} = \omega_n |P| e^{i(\Phi_P + 90^\circ + \epsilon_D)}$$

and

$$\dot{r} = \omega_n |r| e^{i(\Phi_r + 90^\circ + \epsilon_D)}$$

Those relations should be inserted into the expression for n_y. The expression can be solved by:

1. Express n_{y_m}, p, and r as complex variables.
2. Write the equation in terms of real and imaginary quantities by Euler's equation.
3. Perform the indicated multiplications and summations
4. Recombine the real and imaginary quantities into an expression containing an amplitude and a phase.

Ratios of the corrected quantities may be combined with the rules of complex variables. For example,

$$\frac{P}{n_y} = \frac{|P|}{|n_y|} e^{i[\Phi_P - \Phi_{n_y}]} .$$

IV. CONCLUSIONS

The following conclusions may be derived from a consideration of the preceding development and the sample calculations of the analysis presented in the appendix.

1. The time-vector method of analyzing a linear, multiple-degree-of-freedom, oscillatory system is straight-forward and easily applied. It is especially applicable to the analysis of lightly damped systems. It yields relationships between the stability derivatives of an airplane which are commensurate with the accuracy of the transient data. The assumption of reasonable values for some derivatives yields good values for the others. An analogous application of the method to the rolling-subsidence and spiral modes permits a unique solution for all of the derivatives.

2. The method of plotting the transient data provides:

   (a) the period and frequency of the oscillation,

   (b) the damping of the oscillation,

   (c) relationships between the phases and the amplitudes of the oscillatory components.

It also indicates any deviations from linearity. Similarly, it permits the averaging of any experimental scatter which may exist.

3. The method fully exploits the linear qualities of the transient data of a system which may be described mathematically by a set of simultaneous, linear, differential equations.

4. The graphical solution clearly indicates the presence of any inconsistencies in the data. It also assists the engineer in determining the proper adjustment.

5. It was noted that errors due to instrument misalignment or location are significant. A method was developed for correcting those errors.

V. REFERENCES

1. Bryan, G. H., Stability in Aviation, 1911.

2. Duncan, W. J., The Principles of the Control and Stability of Aircraft, Cambridge at the University Press, 1952.

3. Garner, H. M. and Gates, B. A., "Full Scale Determination of the Lateral Derivatives of a Bristol Fighter Airplane," Br. A. R. C. R. and M. 987, 1925.

4. Milliken, W. F., Jr., "Progress in Dynamic Stability and Control Research," Journal of the Aeronautical Sciences, Vol. 14, No. 9, p. 493, September 1947.

5. Milliken, W. F., Jr., "Dynamic Stability and Control Research," Cornell Aeronautical Laboratory Report No. 39, September 1951.

6. Segel, L., "Dynamic Lateral Stability Flight Tests of an F-80A Airplane by the Forced Oscillation and Step Function Response Methods," Cornell Aeronautical Laboratory Report No. TB-495-F-13, April 1950.

7. Greenberg, Harry, "A Survey of Methods for Determining Stability Parameters of an Airplane from Dynamic Flight Test Measurements," NACA Technical Note 2340, U. S. Government Printing Office, April 1951.

8. Shinbrot, M., "A Least-Squares Curve-Fitting Method With Applications to the Calculation Transient Response Data," NACA Technical Note 2341, U. S. Government Printing Office, April 1951.

9. Donegan, J. and Pearson, H. A., "A Matrix Method of Determining the Longitudinal-Stability Coefficients and Frequency Response of and Aircraft from Transient Flight Data," NACA Technical Note 2371, U. S. Government Printing Office, June 1951.

10. Shinbrot, M., "An Analysis of the Errors in Curve-Fitting Problems With Application to the Calculation of Stability Parameters from Flight Data," NACA Technical Note 2820, U. S. Government Printing Office, November 1952.

11. Donegan, J. J., "Matrix Methods for Determining the Longitudinal-Stability Derivatives of an Airplane from Transient Flight Data," NACA Technical Note 2902, U. S. Government Printing Office, March 1953.

12. Mueller, R. K., "The Graphical Solution of Stability Problems," Journal of the Aeronautical Sciences, Vol. 4, p. 324, June 1937.

13. Doetsh, K. H., "The Time-Vector Method for Stability Investigations," Royal Aircraft Establishment Report, Aero 2495, Great Britain.

14. Larrabee, E. E., "Application of the Time-Vector Method to the Analysis of Flight Test Lateral Oscillation Data," Cornell Aeronautical Flight Research Department Memorandum No. 189, Sept. 9, 1953.

VI. APPENDIX

A. Sample Calculations of a Time-Vector Analysis of a Lateral Oscillation

1. General Discussion

The time-vector method was used to extract the lateral stability derivatives of a fighter airplane from its lateral oscillation. A three-view drawing of the airplane is presented on page 59 . The lateral oscillation was excited by a rudder pulse; a representation of the flight record is shown on page 58 .

2. Flight conditions

w = 12,880 lb, $s = 237.6$ ft^2

I_{x_p} = 12,540 slug-ft^2, $b = 38.9$ ft

I_{z_p} = 31,000 slug-ft^2

C. G. position: 25.6% M. A. C.

Altitude: 20,000 ft

V_i = 260 MPH

OAT = +3^{o}F

3. Calculation of flight constants

(a) It must be assumed that $V_i = V_c$ since no airspeed calibration data were available.

Then,

$$M = .493$$
$$V_o = Ma$$
$$= (.493)(1116)(.944)$$
$$= \underline{\underline{519}} \text{ ft/sec}$$

(b) $C_{L_o} = \frac{w}{1481\ M^2\ \delta S}$

$= \frac{12,880}{(1481)(.493)^2(.459)(237.6)}$

$= \underline{\underline{.328}}$

(c) $\mu_o = \frac{m}{\rho_o S b}$

$= \frac{12,880}{(32.2)(.002378)(237.6)(38.9)}$

$= \underline{\underline{18.18}}$

(d) $\tau_o = \frac{b}{\sqrt{\sigma}\, V_o}$

$= \frac{38.9}{(.718)(519)}$

$= \underline{\underline{.1045 \text{ sec}}}$

4. Flight attitude

Flight measurements indicated that $\theta_{o_L} = -1.7^o$

$\frac{\partial C_L}{\partial \alpha} = 5.10$ per radian

$= \frac{5.10}{57.3}$

$= .089$ per degree

Then $$\theta = \frac{C_{L_o}}{\left(\frac{\partial C_L}{\partial \alpha}\right)} + \theta_{o_L}$$

$$= \frac{.328}{.089} - 1.7$$

$$= 3.69 - 1.7$$

$$\theta = \underline{\underline{2^o}}$$

The X principal axis of inertia is estimated 4^o below the reference axis of the airplane.

$\eta = +2^o$.

5. Inertia constants

$$K_{x_p}^2 = \left(\frac{1}{b}\right)^2 \left(\frac{I_{x_p}}{m}\right)$$

$$= \frac{(12540)(32.2)}{(38.9)^2(12880)}$$

$$= \underline{\underline{.0207}}$$

$$K_{z_p}^2 = \left(\frac{1}{b}\right)^2 \left(\frac{I_{z_p}}{m}\right)$$

$$= \frac{(31,000)(32.2)}{(38.9)^2(12880)}$$

$$= \underline{\underline{.0512}}$$

For $\eta = +2^o$

$$K_x^2 = K_{x_p}^2 \cos^2\eta + K_{z_p}^2 \sin^2\eta$$

$$K_x^2 = (.0207)(\cos 2^o)^2 + (.0512)(\sin 2^o)^2$$

$$= .0207 + .0000624$$

$$= \underline{\underline{.0208}}$$

$$K_z^2 = K_{z_p}^2 \cos^2 \eta + K_{x_p}^2 \sin^2 \eta$$

$$= (.0512)(\cos 2^o)^2 + (.0207)(\sin 2^o)^2$$

$$= .0512 + .000,025,2$$

$$= \underline{\underline{.0512}}$$

$$K_{xz} = (K_{z_p}^2 - K_{x_p}^2) \sin \eta \cos \eta$$

$$= (.0512 - .0207) \sin 2^o \cos 2^o$$

$$= \underline{\underline{.001,064}}$$

6. Analysis of the time-histories of the oscillations

The curves on page 60 yield the following information:

(a) the frequency of the lateral oscillation,

(b) the phase relationship between degrees of freedom,

The curves on page 61 provide:

(a) the amount of damping present in the oscillation,

(b) the relative magnitudes of the components of the lateral oscillation.

From those curves

$\zeta = .0998,$ $\omega = 2.17 \frac{\text{rad}}{\text{sec}}$

Table 1, Measured Phase and Amplitude Relationships

Measured Quantity	Amplitude Relationships	Phase Angle Relationships
p	.0664 rad/sec	144.3 deg.
r	.0736 rad/sec	265.5 deg.
n_y	.0218 g's	180 deg.

Those relationships must be corrected for the orientation of the input axes of the roll rate and yaw rate gyros, and for the location of the lateral accellerometer with reference to the airplane center of gravity. The instrument orientations and locations are shown below.

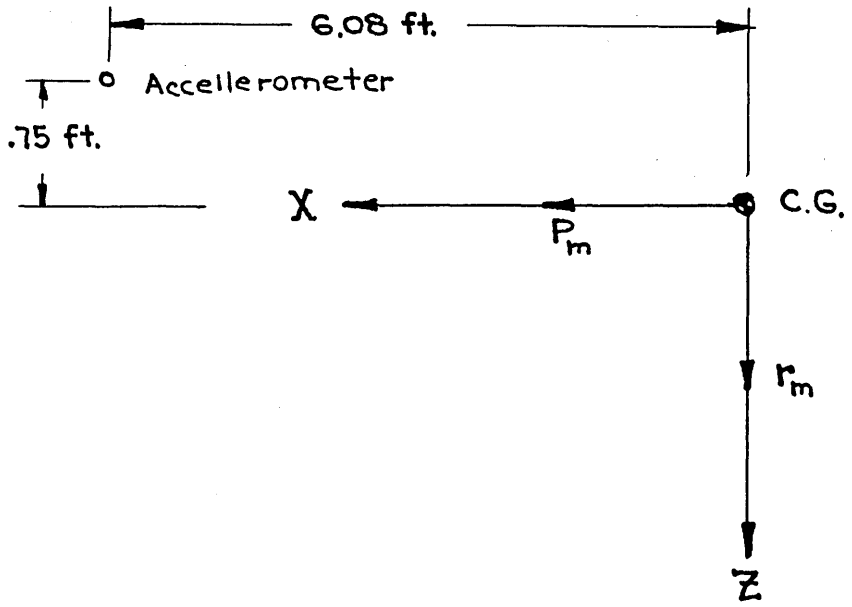

Fig. 11, Fighter Airplane instrument Geometry

$p = p_m$ $\qquad D = \sin - \zeta$

$p = r_m$ $\qquad = \underline{5.8^o}$

$$n_y = n_{y_m} - \frac{.75}{g}\dot{p} - \frac{6.08}{g}\dot{r}$$

$$\dot{p} = \omega_n |p| e^{i(\Phi_p + 90^o + \epsilon_D)}$$

$$= (2.17 \text{ rad/sec})(.0664) e^{i(144.3 + 90 + 5.8)}$$

$$= \underline{.144} \text{ rad/sec}^2 \text{ at } 240.1^o$$

$$\dot{r} = \omega_n |r| e^{i(\Phi_r + 90^o + \epsilon_D)}$$

$$= (2.17 \text{ rad/sec})(.0736) e^{i(265.5 + 90 + 5.8)}$$

$$= \underline{.159} \text{ rad/sec}^2 \text{ at } + 1.3^o$$

$$n_y = n_{y_m} - \frac{(.75)(.144)}{32.2} e^{i(240.1^o)} - \frac{(6.08)(.159)}{32.2} e^{i(1.3^o)}$$

$$= .0218\, e^{i(180^o)} - .00336\, e^{i(240.1^o)} - .0300\, e^{i(1.3^o)}$$

$$= \underline{.0502} \text{ at } \underline{177.5^o}$$

Fig. 12 shows the vector relationships before and after correction for the instrument orientations and location.

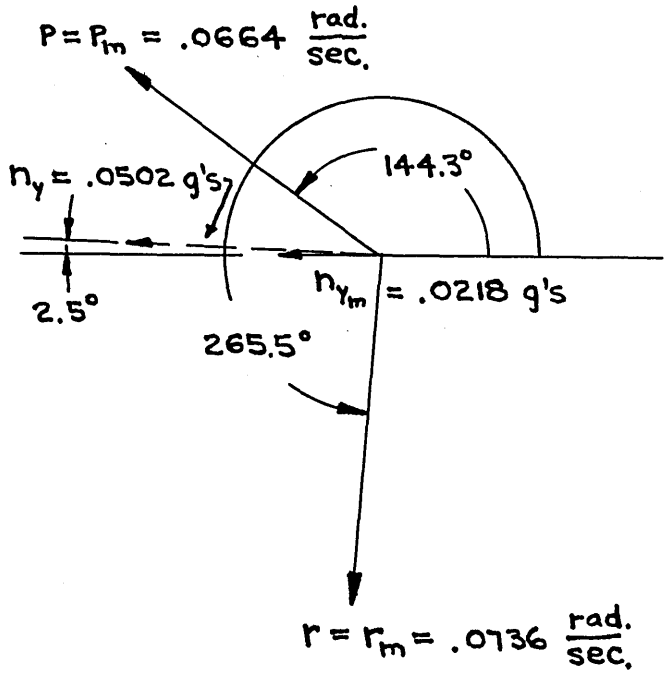

Fig. 12, Phase and Amplitude Correction

Rotation of the vector diagram so that the phase of n_y is 180^o gives:

Table 2, Corrected Phase and Amplitude Relationships

Quan.	Amplitude	Phase
p	.0664 rad/sec	146.8
r	.0736 rad/sec	268
n_y	.0502 g's	180^o

The angular velocities must be nondimensionalized for insertion into the equations of motion presented on page 12 .

$$p = \frac{d\phi}{dt}$$

$$D\phi = \frac{d\phi}{d(t/\tau_o)}$$

$$= \tau_o \frac{d\phi}{dt}$$

$$= (.1045 \text{ sec})(.0664 \text{ rad/sec})$$

$$= \underline{.00694} \text{ at } 146.8^o$$

$$D\psi = \tau_o \frac{d\psi}{dt} = \tau_o r$$

$$= (.1045)(.0736)$$

$$= \underline{.00770} \text{ at } 268^o$$

$$'\omega_n = \tau_o \omega_n$$

$$= (.1045)(2.17)$$

$$= \underline{.226}$$

Those relationships, with the nondimensional lateral accelleration should be suitable for use in the final solution of the problem.

7. Discussion of the validity of preceding results

A preliminary analysis, including diagrams, indicated that the supporting data and the actual transient recrods were not compatible. An extensive check of the supporting data, such as airplane weight, inertias, instrument locations, calibrations, and dynamics, was in order. Unfortunately, the flight test had been conducted in 1951; therefore, it was not possible to accomplish those checks. It then became necessary to determine the most logical correction to the data which would be consistent with the transient records and with information on the stability derivatives obtained from other sources.

A study indicated that the following changes were most probable:

(a) n_y = .0073 instead of .0502

(b) k_z = 8.81 ft. instead of 9.85 ft.

(c) k_x = 5.60 ft. instead of 5.69 ft.

Those changes can be shown to be reasonable.

The lateral accelleration could have been inaccurate for one or more of the following reasons:

(a) The instrument calibration could have been incorrect.

(b) Improper excitation voltage may have been used when the test condition was recorded.

(c) The accellerometer location relative to the airplane C.G. may not have been accurately known.

(d) The accellerometer input axis may have been misaligned.

Moments of inertia have very significant effects on the damping and the period of the lateral oscillation. An accurate knowledge of the inertias is thus important. The inertia data received with the flight test records were not considered especially accurate. It became apparent in the analysis that either I_z of the damping of the oscillation had to be reduced in order to obtain reasonable yawing moment derivatives from the rest records. Determination of the damping of the oscillation from the time-histories was straight-forward and considered reliable. Consequently, the airplane moment of inertia about the Z-axis had to be reduced. There are no independent inertia data for the airplane considered which are available for a check. However, the corrected inertias appear reasonable when compared to those of geometrically similar airplane.

8. Calculation of the stability derivatives by means of vector diagrams

(a) Side-force diagram

From page 12 , the side-force equation is:

$$\frac{2\mu_o}{\sqrt{\sigma}} D\beta = C_{y_\beta}\beta + C_{L_o}\,\phi + 2\,\frac{\mu_o}{\sqrt{\sigma}}\,D\psi$$

$$\phi = \frac{|D\phi|}{\omega_n} e^{i\left(\Phi_{D\phi} - 90^o - \epsilon_D\right)}$$

$$= \frac{.00694}{.226} e^{i\,(146.8 - 90 - 5.8)}$$

$$= \underline{\underline{.037}} \text{ at } 51.0^o$$

$$C_{L_o}\,\phi = (.328)(.0307)$$

$$= \underline{.01007} \text{ at } \underline{51.0^o}$$

$$\frac{2\mu_o}{\sqrt{\sigma}} D\psi = \frac{(2)(18.2)}{.718}(.00770)$$

$$= \underline{.390} \text{ at } 268^o$$ (The phase angle will be checked in the diagram).

$$\frac{2\mu_o}{\sqrt{\sigma}} D\beta = \frac{(2)(18.2)}{.718}\,D\beta$$

$$= \underline{50.6\,D\beta}$$

Since side force is almost entirely a result of sideslip, it is reasonable to assume that n_y and β have a phase difference of 180^o. Then, the phase

angle of $D\beta$ is:

$$\Phi_{D\beta} = \Phi_{\beta} + 90^{o} + \epsilon_{D}$$

$$= 0 + 90^{o} + 5.8^{o}$$

$$= \underline{95.8^{o}}$$

Continuing with the assumption proposed above,

$$C_{y_{\beta}}\beta = C_{L_{o}} n_{y}$$

$$= (.328)(.0773)$$

$$= \underline{.0254} \text{ at } \underline{180^{o}}$$

With the information from the side-force diagram,

$$C_{y_{\beta}} = \frac{.0254}{|\beta|} \text{ at } 180^{o}$$

$$= \frac{-.0254}{.0348}$$

$$= \underline{\underline{-.730}}$$

It was necessary to change the phase of $D\psi$ with respect to β from 268^{o} to 273.1^{o} in order to close the vector diagram. It is most reasonable to assume that the phase relationship between $D\phi$ and $D\psi$ was correct as measured. Both quantities were measured by rate gyros with inputs of the same order of magnitude. The lateral accelleration was measured by an accellerometer. Its dynamic response characteristics could be expected to differ from those of the rate gyros. The instruments were

$$D\beta = \frac{.399}{50.6}$$

$$= \underline{\underline{.00788}}$$

$$\beta = \frac{|D\beta|}{\omega_n}$$

$$= \frac{.00788}{.226}$$

$$= \underline{\underline{.0348}} \text{ at } 0°$$

$$\Phi_{D\psi} = \underline{\underline{273.1}}°$$

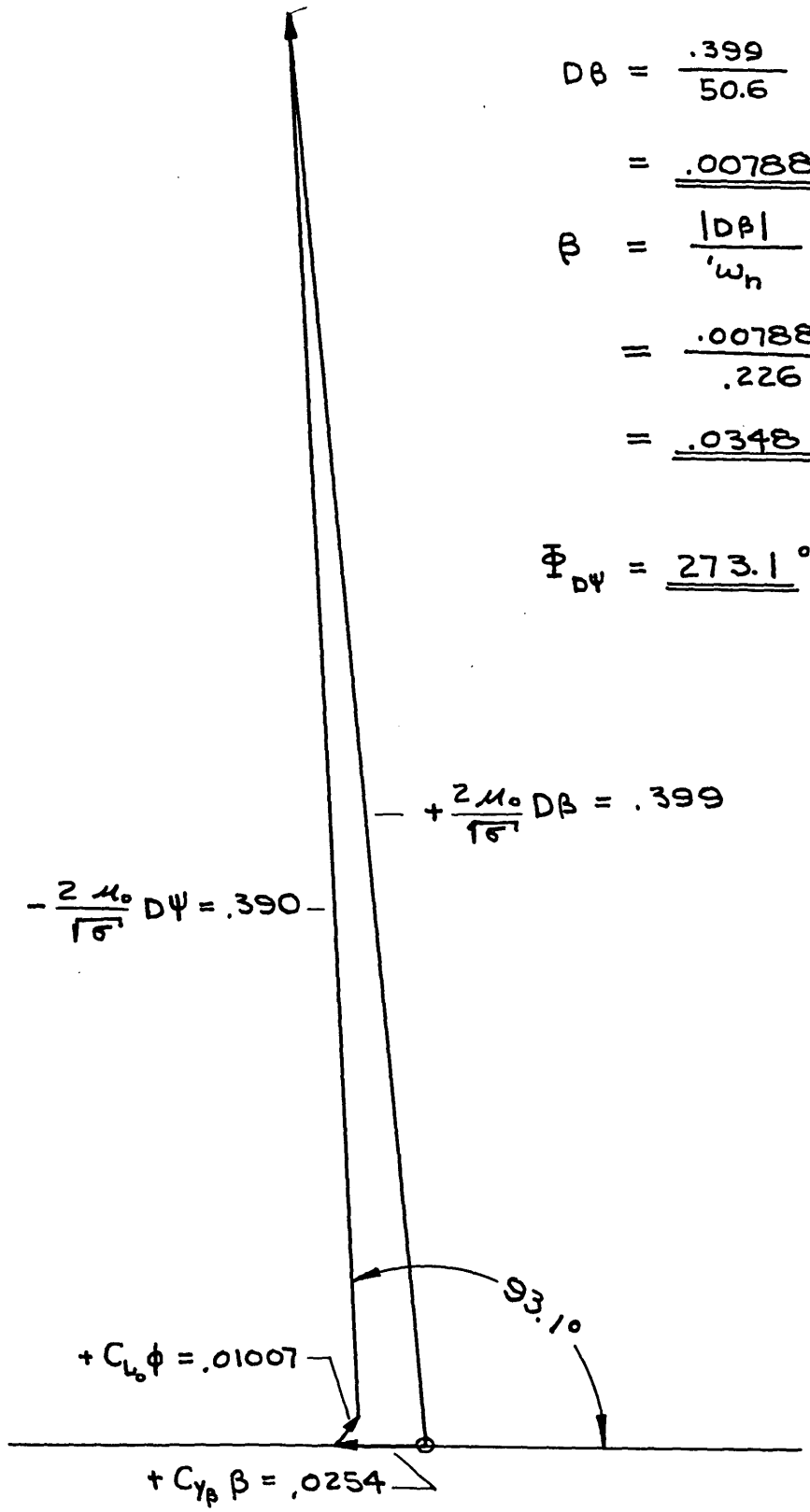

Fig. 13, Side-force vector diagram

selected to provide good dynamic response in the frequency spectrum anticipated for the flight test. However, it should be noted that authorities estimate that an accuracy on the order of $\pm 3^{o}$ in phase response is considered reasonable for the type of instrumentation used. Then,

$$\Phi_{[D\psi;\ \beta]} = 273.1^{o}$$

$$\Phi_{[D\phi;\beta]} = 151.9^{o}$$

$$\Phi_{[n_y;\beta]} = 180^{o}$$

(b) Rolling-moment diagram.

From page 12 , the rolling moment equation is:

$$2\mu_o K_x^2 D^2\phi - \frac{\sqrt{\sigma}}{2} C_{\ell_r} D\psi + 2\mu_o K_{xz} D^2\psi = \frac{\sqrt{\sigma}}{2} C_{\ell_p} D\phi + C_{\ell_\beta}\beta$$

$$\text{Estimate } C_{\ell_r} = +\frac{C_{L_o}}{4}$$

$$= \frac{.328}{4}$$

$$= \underline{.082}$$

The terms in the equation are:

$$D^2\phi = {}'\omega_n \left|D\phi\right| e^{i\left(\Phi_{D\phi} + 90^{o} + 5.8\right)}$$

$$= (.226)(.00694)\, e^{i\left(151.9 + 90 + 5.8\right)}$$

$$= \underline{.001568} \text{ at } \underline{247.7^{o}}$$

$$D^2\psi = (.226)(.00770)\, e^{i\,(273.1 + 90 + 5.8)}$$

$$= \underline{.00174 \text{ at } 8.9^\circ}$$

$$2\mu_o K_x^2 D^2\phi = (2)\ 18.2)(.0208)(.001568)$$

$$= \underline{.001,187} \text{ at } 247.7^\circ$$

$$\frac{\rho}{2} C_{\ell_r} D\psi = \frac{(.718)(.0802)(.00770)}{2}$$

$$= \underline{\underline{.000,226}} \text{ at } 273.1^\circ$$

$$2\mu_o K_{xz} D^2\psi = (2)(18.2)(.001,064)(.001,74)$$

$$= \underline{.000,067,5} \text{ at } 8.9^\circ$$

$$\frac{\rho}{2} C_{\ell_p} D\phi = \frac{(.718)(.00694)}{2}\ C_{\ell_p}$$

$$= \underline{\underline{.00249}}\ C_{\ell_p} \text{ at } 151.9^\circ$$

$$C_{\ell_\beta}\,\beta = \underline{\underline{.0348}}\ C_{\ell_\beta} \text{ at } 0^\circ$$

The rolling-moment vector diagram yielded:

$$C_{\ell_p} = -.527 \qquad \text{(estimated)}$$

$$C_{\ell_\beta} = -.0462$$

$$= 143.5^\circ$$

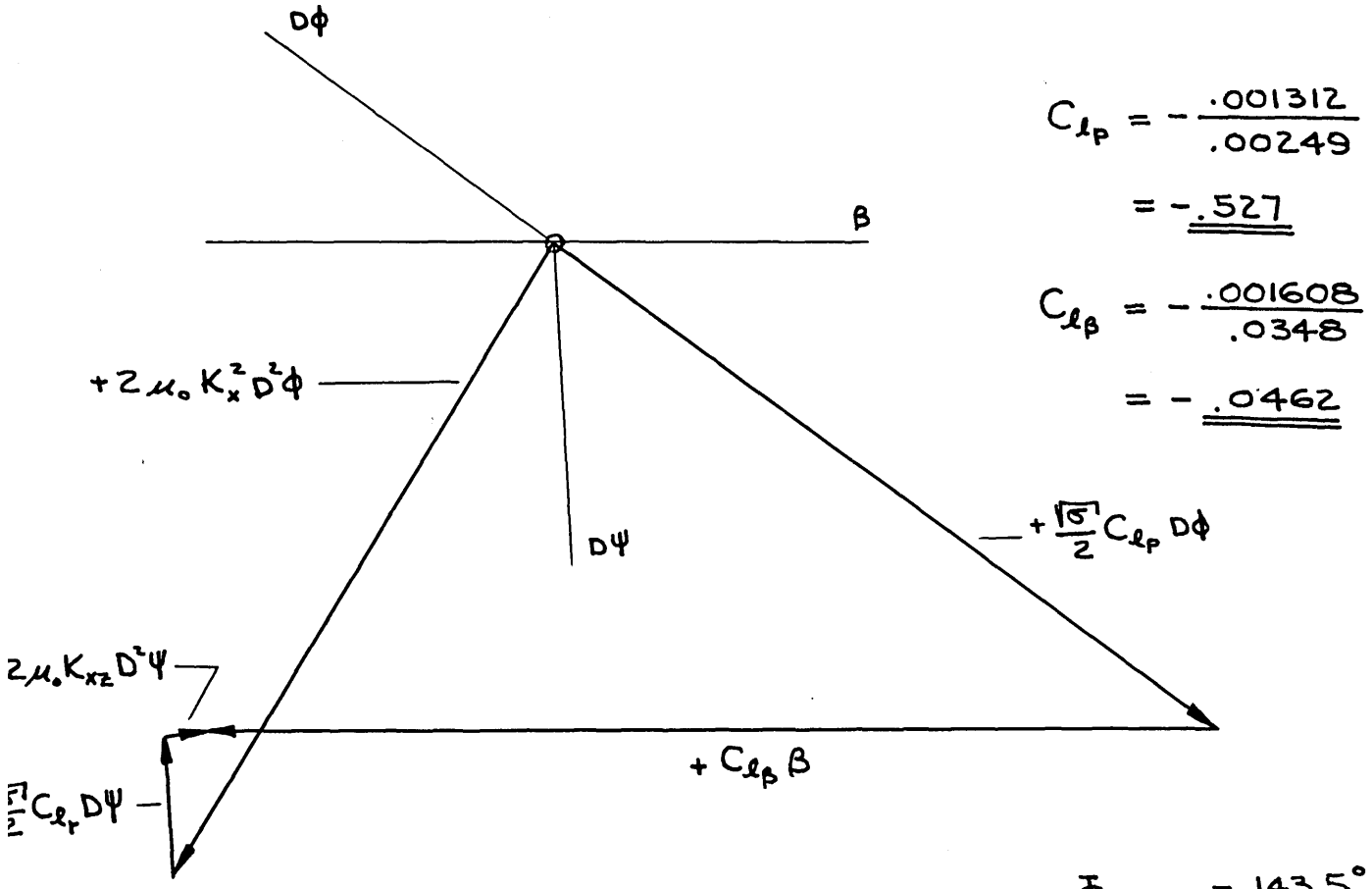

Fig. 14, Rolling-moment Vector Diagram.

The initial construction of the vector diagram using the numbers developed on page 44 yielded an unreasonably high magnitude of C_{ℓ_p}. A study of the rolling moment equation and the vector diagram indicated that the $\Phi_{[D\phi;\beta]}$ was most probably in error. C_{ℓ_p} can be estimated with good accuracy by well-established methods. Introduction of a value for C_{ℓ_p} into the vector diagram permits the solution of C_{ℓ_β} and the correction magnitude of $\Phi_{[D\phi;\beta]}$.

Phase angle errors should be reduced to the minimum instrument errors by a careful selection of instruments and a precise knowledge of the installation orientations and locations. It is again noted that the present data were recorded three and one-half years before analysis. Checks which normally would be accomplished immediately after noting unexpected errors were impossible. It has been noted that a misalignment of the input axes to the rate gyros as shown in Fig. 15 could account for the entire change in the phase of $D\phi$ with respect to $D\psi$. Actually, a major part of the error could be due to instrument dynamic phase response errors.

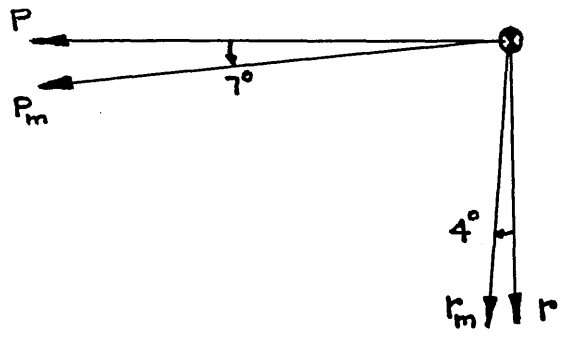

Fig. 15, Phase Corrections

(c) Yawing-moment diagram

From page 12, the yawing-moment equation is:

$$2\mu_o K_z^2 D^2\psi + 2\mu_o K_{xz} D^2\phi - \frac{\sqrt{\sigma}}{2} C_{n_r} D\psi = \frac{\sqrt{\sigma}}{2} C_{n_p} D\phi + C_{n_\beta}\beta$$

Again, one derivative must be estimated. For the airplane considered, $C_{n_p} \cong 0$.

$D^2\psi = .00174$ at $8.9°$

$D^2\phi = .001568$ at $239.3°$

$D\psi = .00770$ at $273.1°$

$\beta = .0348$ at $0°$

$2\mu_o K_z^2 D^2\psi = (2)(18.2)(.052)(.00174)$

$= .00325$ at $8.9°$

$2\mu_o K_{xz} D^2\phi = (2)(18.2)(.001064)(.001523)$

$= .000,060,6$ at $239.3°$

$\frac{\sqrt{\sigma}}{2} C_{n_r} D\psi = \frac{(.718)(.00770)}{2} C_{n_r}$

$= .00276\, C_{n_r}$ at $273.1°$

$C_{n_\beta}\beta = .0348\,\beta$ at $0°$

9. Summary of Results

The stability derivatives derived from the flight test are compared with the manufacturer's estimates in Table 3.

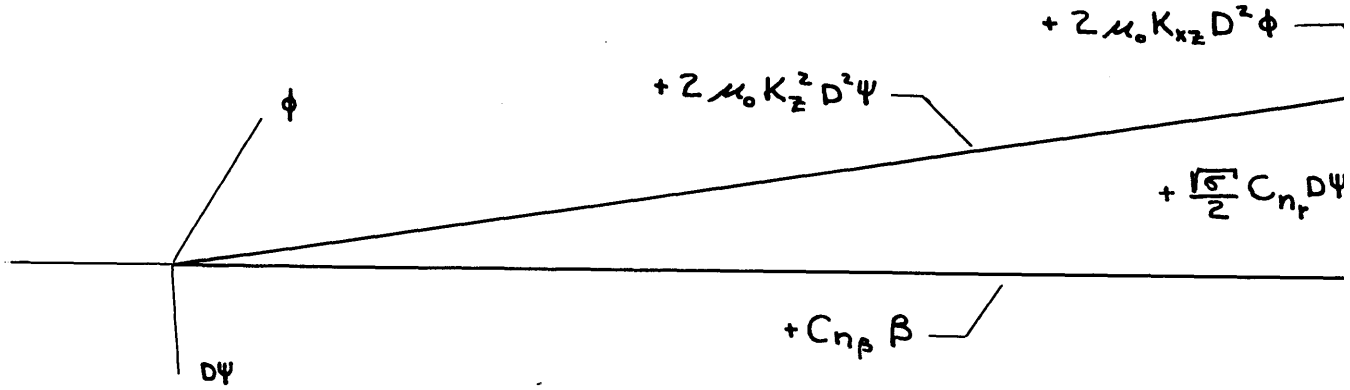

$$C_{n_r} = -\frac{.00441}{.00276}$$

$$= \underline{\underline{-.160}}$$

$$C_{n_\beta} = \frac{.003,207}{.0348}$$

$$= \underline{\underline{.0922}}$$

Fig. 16, Yawing-moment vector diagram.

Table 3, Comparison Between Extracted and Derivatives and Manufacturer's Estimates

Source	Time-Vector Analysis	Manufacturer's Estimates
Mach No.	.50	.60
Altitude	20,000 ft	20,000 ft
Weight	12,800 lb	14,500 lb
C.G. pos.	25.6% M.A.C.	27% M.A.C.
I_x	12,540	26,400
I_z	31,000	52,200
C_{y_β}	-.73	-.788
C_{ℓ_β}	-.0462	-.066
C_{ℓ_p}	-.527	-.545
C_{ℓ_r}	.082 (est)	.065
C_{n_β}	.0922	.093
C_{n_p}	0 (est)	.015
C_{n_r}	-.160	-.136

Some additional information which were obtained from the transient analysis are:

$$\frac{|\beta|}{\left|\frac{Pb}{2V_o}\right|} = 13.98 \qquad \zeta = .0998$$

$$\frac{|\beta|}{\left|\frac{rb}{2V_o}\right|} = 12.60 \qquad \omega = 2.16 \ \frac{\text{rad.}}{\text{sec.}}$$

$$\frac{|\beta|}{|n_y|} = 25.8 \ \frac{deg.}{g}$$

B. Lateral Oscillation Analysis by the Method of Ref. 6

The same rudder-pulse flight condition has been investigated using the method of Ref. 6. It was not possible to determine all of the stability derivatives since the airplane oscillation was not excited in the manner most appropriate to that method of analysis.

The equations presented below have been taken from pages 19 and 20 of Ref. 6. The nomenclature has been changed to correspond to that of this paper.

$$\lambda_z = \frac{\mu_0 C_{\ell_p} C_{n_\beta}}{(8\sigma)(K_x^2 K_z^2 - K_{xz}^2)(\omega_n^2)(\frac{\mu_0}{\sqrt{\sigma}} \tau_0)^3}$$

C_{ℓ_p} must be known. The method of Ref. 6 relies upon th measurement of the sideslip angle. The value obtained by the vector method will be used in this analysis

$$\lambda_z = \frac{\mu_0 C_{\ell_p} C_{n_\beta} = (18.2)(-.527) C_{n_\beta}}{[(8)(.516)][(.028)(.0512)(-(.001064)^2][2.17]^2[\frac{(18.2)}{.718}(.1045)]^3}$$

$$= -24.8 \ C_{n_\beta}$$

$$4(K_x^2 K_z^2 - K_{xz}^2)(\lambda_z - 2\xi\omega_n)(\frac{\mu_0}{\sqrt{\sigma}} \tau_0) =$$

$$K_x^2(2K_z^2 C_{y_\beta} + C_{n_r} + K_{xz}^2 C_{\ell_p})$$

$$4[.001065][-24.8\,C_{n_\beta} - (2)(.218)][2.65] =$$

$$[.0208][(2)(.0512)(-.73) + C_{n_r}] + [.0512][-.527]$$

$$-.280\,C_{n_\beta} - .0208\,C_{n_r} = -.0235$$

$$C_{n_\beta} + .0744\,C_{n_r} = .0840$$

$$16[K_x^2 K_z^2 - K_{xz}^2][-2\zeta\omega_n\lambda_z + \omega_n^2]\left[\frac{\mu_o}{\sqrt{\sigma}}\tau_o\right]^2 =$$

$$C_{n_r}[C_{l_p} + 2K_x^2 C_{y_\beta}] + \frac{8\mu_o K_x^2 C_{n_\beta}}{\sigma} + 2K_z^2 C_{y_\beta} C_{l_p}$$

$$16[.001065][(-.436)(-24.8C_{n_\beta}) + (2.17)^2][2.65]^2 =$$

$$C_{n_r}[-.527 + (2)(.0208)(-.73)] + \frac{(8)(18.2)(.0208)}{.516} C_{n_\beta} +$$

$$+ (2)(.0512)(-.73)(-.527)$$

$$-.458\,C_{n_\beta} + .557\,C_{n_r} = -.524$$

$$C_{n_\beta} - .1218\,C_{n_r} = .1143$$

The value for C_{y_β} was obtained in the manner shown on page 42 .

$$C_{n_\beta} = \frac{\begin{vmatrix} .0840 & .0744 \\ .1143 & -.1218 \end{vmatrix}}{\begin{vmatrix} 1 & .0744 \\ 1 & -.1218 \end{vmatrix}} = \frac{-.01873}{-.1962}$$

$$= +.0955$$

$$C_{n_r} = \frac{\begin{vmatrix} 1 & .0840 \\ 1 & .1143 \end{vmatrix}}{\begin{vmatrix} 1 & .0744 \\ 1 & -.1218 \end{vmatrix}} = \frac{.0303}{-.1962}$$

$$= -.1543$$

The solutions are seen to compare very well with those obtained by the time-vector method.

Table 4, Comparison Between Derivatives Extracted by Time-Vector and Ref. 5 Methods

Method	Time-Vector	Ref. 6
C_{n_β}	.0922	.0955
C_{n_r}	-.160	-.1543

C. Rolling Subsidence Mode Analysis With Sample Calculations

The contribution of roll to the lateral oscillation considered in the preceding analysis was small. The relatively small magnitudes of the stability derivatives, C_{ℓ_β} and C_{ℓ_r}, were responsible. The separation of the rolling-subsidence mode from the lateral oscillation was not feasible.

A second test condition performed by the same airplane was considered. Since the transient was initiated with an aileron pulse, a relatively high roll rate was imposed at the beginning of the maneuver. After the ailerons were returned to neutral, the maneuver was dominated by the rolling-subsidence mode for approximately one second.

The test conditions are summarized below. Since similar parameters were developed in detail for the lateral oscillation study, only the results are listed.

$w = 13,830$ lb

$K_x^2 = .0273$

$V_i = 315$ MPH

$M = .592$

ALT = 20,000 ft

$C_{L_o} = .244$

$\mu_o = 19.6$

$\tau_o = .0869$

$V_o = 625$ ft/sec

The analysis to be used assumes that only the rolling component is significant in the rolling-subsidence mode. That assumption is justified by:

1. The initial roll rate is very large relative to the other motions.

2. C_{l_β} and C_{n_p} are relatively small for the airplane considered. $C_{n_p} \cong 0$.

It may be noted from the curves on page 58 that over-control occurred when the ailerons were returned to neutral. The aileron application opposite to the roll direction acted with the damping in roll and must be considered.

With the assumption that only rolling motion was significant, the present analysis could have been completed without quantitative knowledge of instrument sensitivities if aileron over-control had not occurred. However, it is necessary to know the aileron setting in order to ascertain the contribution of the ailerons to the damping. Unfortunately, the instrument sensitivity information for that particular test has been lost. It is again noted that the tests were conducted in 1951.

Although the aileron over-control was small relative to the magnitude of the pulse, its effect was significant. It was determined that an initial total aileron angle over-control of one-half of one degree, as shown on page 56 , provides a correction which gives a reasonable value for C_{l_p}

The equation for pure rolling may be written

$$\left[2\mu_o K_x^2 D^2 - \frac{\sqrt{\sigma}}{2} C_{l_p} D\right] \phi = C_{l_{\delta a}} \delta a$$

where $$D^2 = \frac{d^2}{d\left(\frac{t}{\tau_o}\right)^2}$$

$$\delta a = \delta a_o \left(1 - \frac{t}{T}\right)$$

An expression relating p and C_{l_p} is desired, where

$$P = \frac{d\phi}{dt} = \tau_o D\phi$$

Solution of the differential equation for p gives:

$$P = \left[\frac{C_{l_{\delta a}} \delta a_o}{\frac{\sqrt{\sigma}}{2} \tau_o C_{l_p}}\right]\left[\frac{t}{T} - 1 + \frac{2\mu_o K_x^2 \tau_o}{\frac{\sqrt{\sigma}}{2} C_{l_p} T}\right] + \text{CONST. } e^{\left(\frac{\frac{\sqrt{\sigma}}{2} C_{l_p}}{2\mu_o K_x^2 \tau_o}\right) t}$$

The constant can be evaluated with the initial condition, at t = 0, p = 2.05 inches of trace deflection. After substitution,

$$P = \left[\frac{C_{l_{\delta a}} \delta a_o}{\frac{\sqrt{\sigma}}{2} \tau_o C_{l_p}}\right]\left[-1 + \frac{t}{T} + \frac{2\mu_o K_x^2 \tau_o}{\frac{\sqrt{\sigma}}{2} C_{l_p} \tau_o}\right] +$$

$$+ \left[2.05 - \frac{C_{l_{\delta a}} \delta a_o}{\frac{\sqrt{\sigma}}{2} \tau_o C_{l_p}}\left\{-1 + \frac{2\mu_o K_x^2 \tau_o}{\frac{\sqrt{\sigma}}{2} C_{l_p} T}\right\}\right] e^{\left(\frac{\frac{\sqrt{\sigma}}{2} C_{l_p}}{2\mu_o K_x^2 \tau_o}\right) t}$$

By inserting the values

$\mu_o = 39.2$

$K_x^2 = .0273$

$T = .5$ sec

$\sqrt{\sigma} = .716$

$\tau_o = .0869$

$C_{l_{\delta_a}} = -.126$ per radian

$\delta_{a_o} = .5$ degree $= .00873$ rad.

and the condition

$$p = .63 \text{ inches at } t = .5 \text{ sec}$$

the result $C_{\ell_p} = -.53$ is obtained.

Although C_{ℓ_p} compares favorably with the value used in the lateral oscillation, it si obviously not intended as a check. A pre-knowledge of C_{ℓ_p} was necessary to estimate the aileron contribution to the damping-in-roll. It had been expected that the analysis would substantiate the magnitude of C_{ℓ_p} used in the lateral oscillation analysis. Calculations were essentially completed while a search was being conducted for the instrument calibrations. The analysis does illustrate a method for evaluating C_{ℓ_p}. That is the only justification for its inclusion in this report.

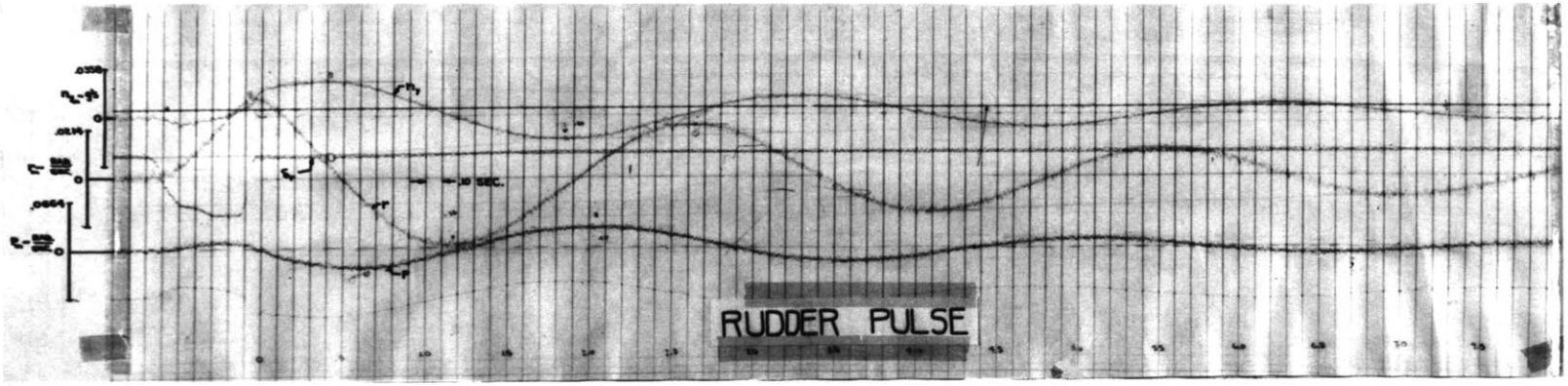

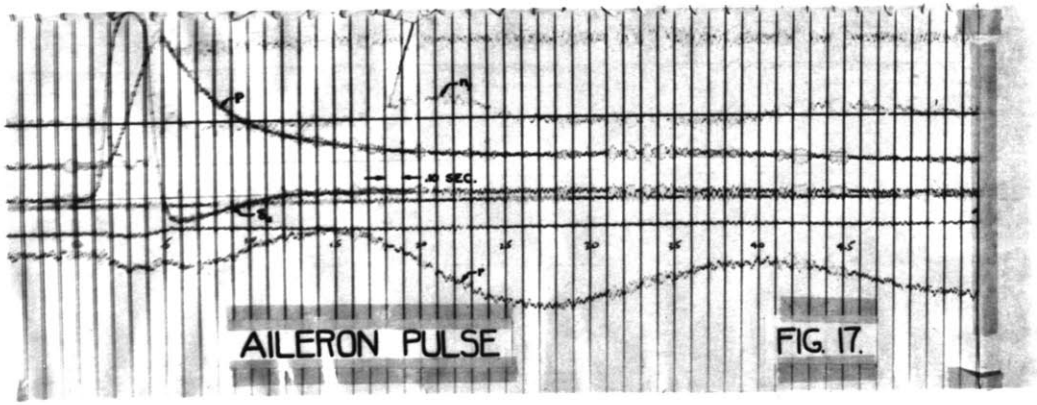

FIG. 17.

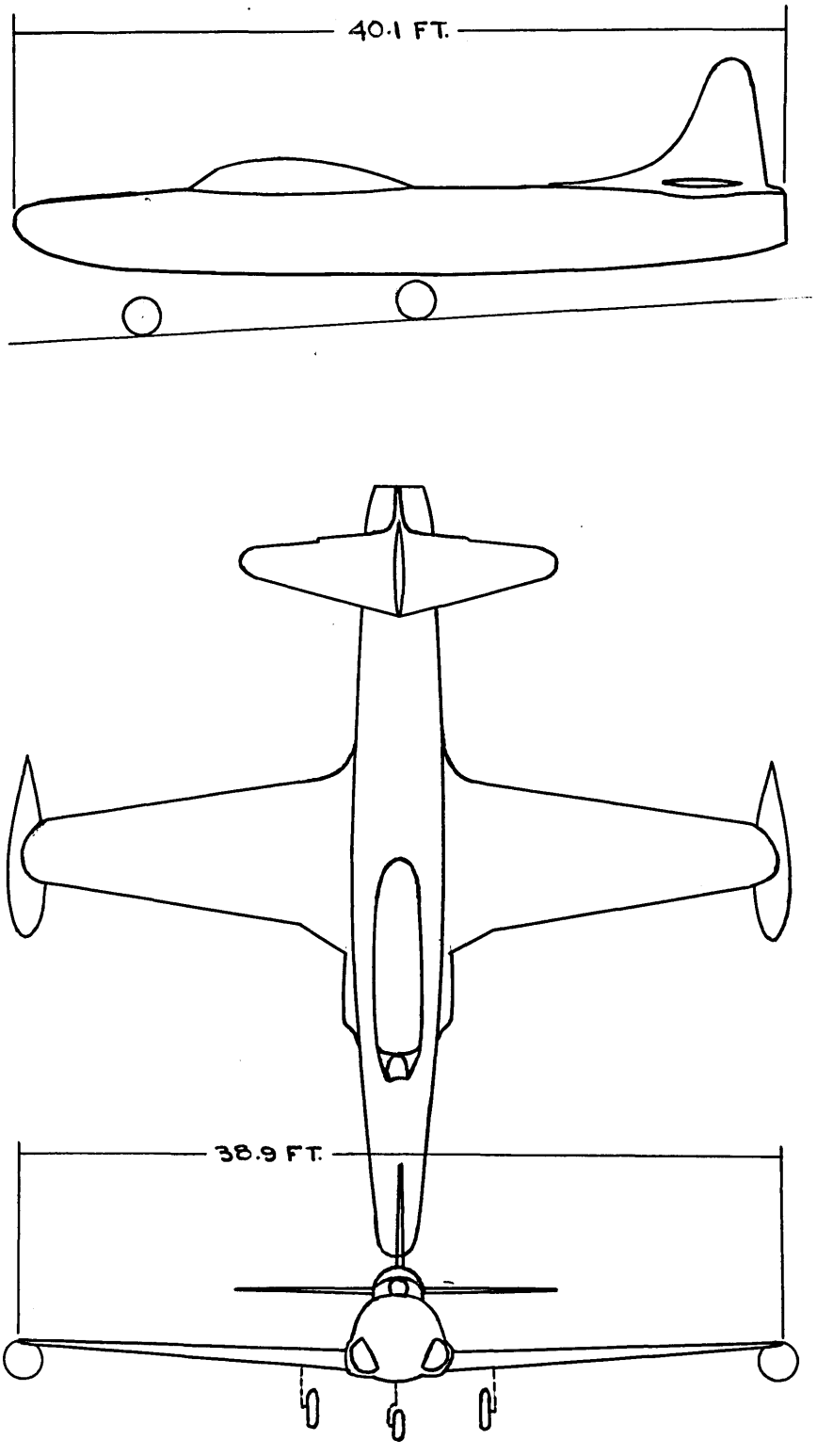

FIG. 18

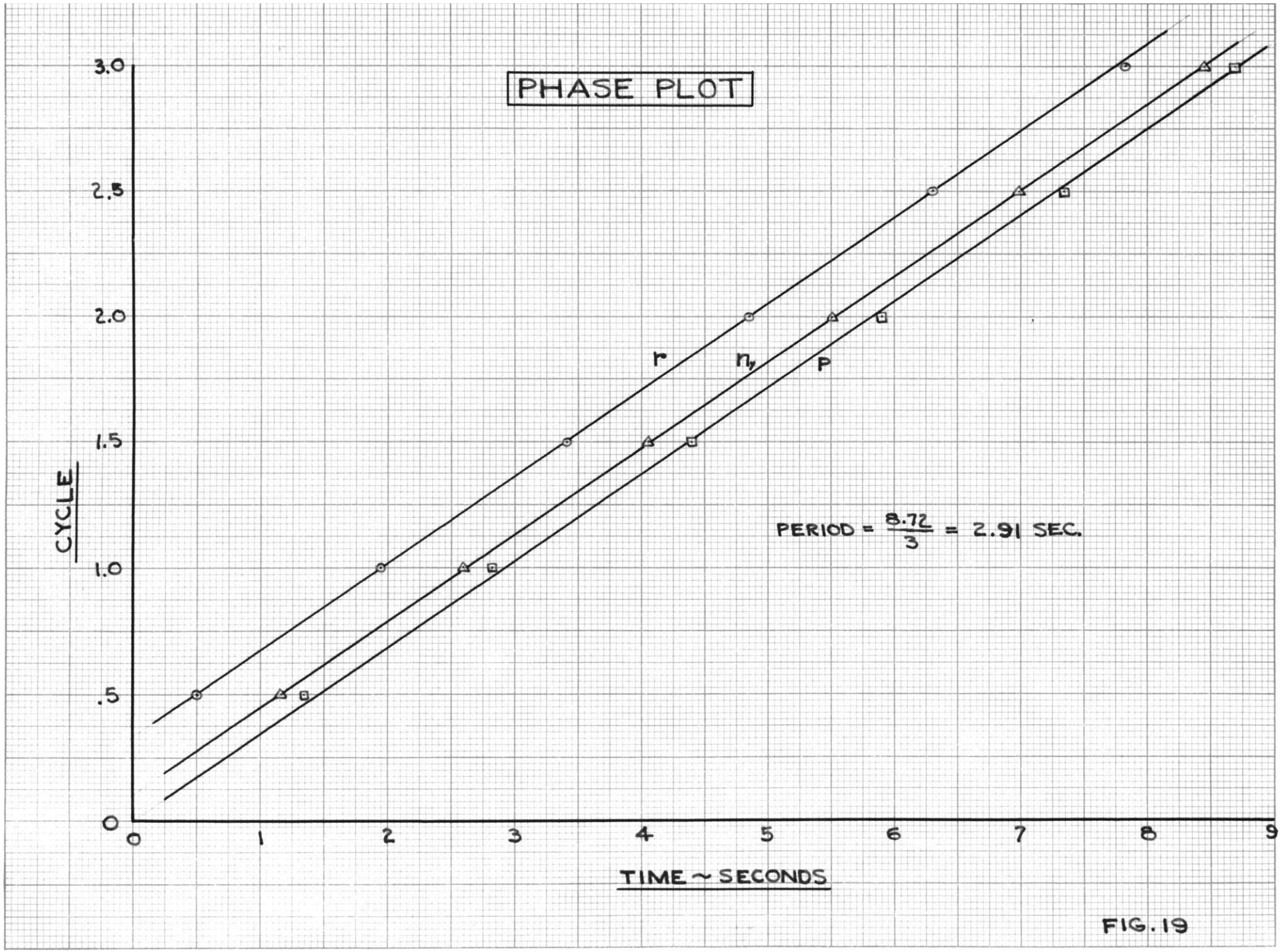
PHASE PLOT
3.0
2.5
2.0
1.5
1.0
.5
0
CYCLE
r
n_y
P
PERIOD = $\frac{8.72}{3}$ = 2.91 SEC.
0
1
2
3
4
5
6
7
8
9
TIME ~ SECONDS

FIG. 19

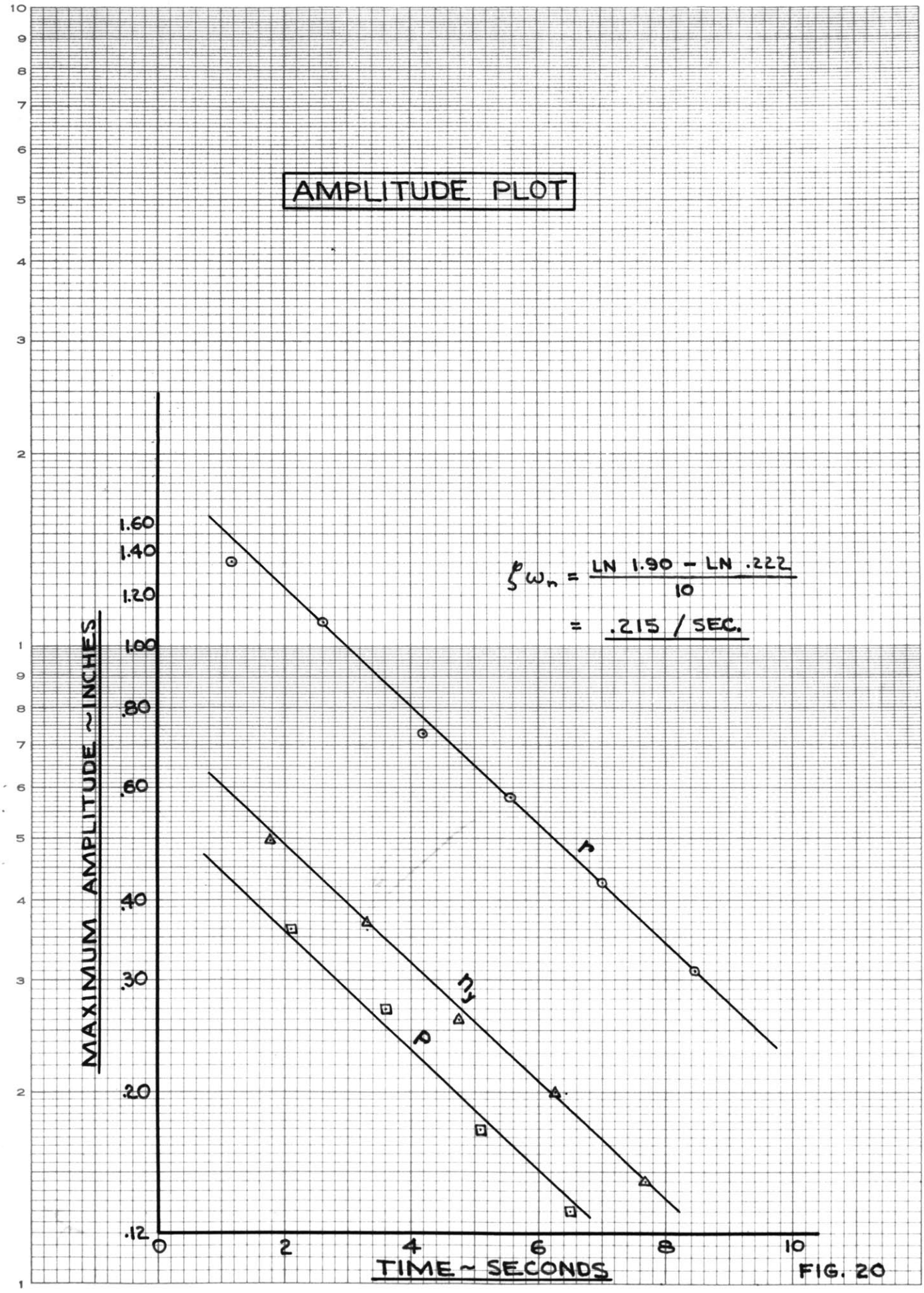
AMPLITUDE PLOT
MAXIMUM AMPLITUDE ~ INCHES
1.60
1.40
1.20
1.00
.80
.60
.40
.30
.20
.12
0
2
4
6
8
10
TIME ~ SECONDS
$\zeta\omega_n = \frac{LN\ 1.90 - LN\ .222}{10}$
$= .215\ /\ SEC.$
R
Ry
P

FIG. 20